



저작자표시-비영리-변경금지 2.0 대한민국

이용자는 아래의 조건을 따르는 경우에 한하여 자유롭게

- 이 저작물을 복제, 배포, 전송, 전시, 공연 및 방송할 수 있습니다.

다음과 같은 조건을 따라야 합니다:



저작자표시. 귀하는 원저작자를 표시하여야 합니다.



비영리. 귀하는 이 저작물을 영리 목적으로 이용할 수 없습니다.



변경금지. 귀하는 이 저작물을 개작, 변형 또는 가공할 수 없습니다.

- 귀하는, 이 저작물의 재이용이나 배포의 경우, 이 저작물에 적용된 이용허락조건을 명확하게 나타내어야 합니다.
- 저작권자로부터 별도의 허가를 받으면 이러한 조건들은 적용되지 않습니다.

저작권법에 따른 이용자의 권리는 위의 내용에 의하여 영향을 받지 않습니다.

이것은 [이용허락규약\(Legal Code\)](#)을 이해하기 쉽게 요약한 것입니다.

[Disclaimer](#)

이학박사 학위논문

Development of an alternative  
calcineurin inhibitor derived from  
CABIN1 peptide

CABIN1 펩타이드를 이용한  
대체 calcineurin 억제제 개발

2022 년 08 월

서울대학교 대학원

분자의학 및 바이오제약전공

이 상 호

# CABIN1 펩타이드를 이용한 대체 calcineurin 억제제 개발

지도교수 윤 홍 덕

이 논문을 이학박사 학위논문으로 제출함  
2022년 08월

서울대학교 대학원  
분자의학 및 바이오제약전공  
이 상 호

이상호의 이학박사 학위논문을 인준함  
2022년 08월

위 원 장 박 경 수 (인)

부위원장 윤 홍 덕 (인)

위 원 이 은 봉 (인)

위 원 정 기 훈 (인)

위 원 장 현 철 (인)

# Development of an alternative calcineurin inhibitor derived from CABIN1 peptide

by  
Sangho Lee

A thesis submitted to the Department of Molecular  
Medicine & Biopharmaceutical Sciences  
for the Degree of Doctor of philosophy in Science  
at Seoul National University Graduate School

August 2022

Approved by Thesis Committee:

Professor     KyongSoo Park     Chairman

Professor     Hong-Duk Youn     Vice chairman

Professor     Eun Bong Lee    

Professor     Keehoon Jung    

Professor     Hyonchol Jang

# ABSTRACT

## Development of an alternative calcineurin inhibitor derived from CABIN1 peptide

Sangho Lee

Department of Molecular Medicine & Biopharmaceutical Sciences  
Graduate School of Convergence Science and Technology

The *C*-terminal fragment of calcineurin binding protein-1 (CABIN1) interacts with calcineurin and represses the transcriptional activity of nuclear factor of activated T cells (NFAT). However, the specific sequences and mechanisms through which it binds to calcineurin are unclear. This study determined that decameric peptide (CABIN1 residues 2146 to 2155) is minimally required for binding to calcineurin. This peptide contains a unique “PPTP” *C*-terminal sequence and a “PxIxIT” *N*-terminal motif. Furthermore, p38 MAPK phosphorylated the threonine residue of the “PPTP” sequence under physiological conditions, dramatically enhancing the peptide’s binding affinity to calcineurin. Therefore, the CABIN1 peptide inhibited the calcineurin–NFAT pathway and the activation of T cells more efficiently than the VIVIT peptide without affecting calcineurin’s phosphatase activity. The CABIN1 peptide could thus be a more potent calcineurin inhibitor and provide therapeutic opportunities for various diseases caused by the calcineurin–NFAT pathway.

Keyword: CABIN1, T cell, Calcineurin, NFAT, VIVIT, p38 MAPK

Student Number: 2017-32606

# TABLE OF CONTENTS

ABSTRACT.....	i
TABLE OF CONTENTS .....	iii
LIST OF FIGURES.....	iv
LIST OF ABBREVIATIONS .....	viii
I . INTRODUCTION.....	1
II . MATERIALS AND METHODS .....	11
III. RESULTS .....	25
IV. DISCUSSION .....	71
V . REFERENCES .....	79
VI. ABSTRACT IN KOREAN.....	90

## LIST OF FIGURES

Figure 1 Domain composition and mechanism of activation of calcineurin.....	4
Figure 2 Major T cell signaling pathways for activation .....	6
Figure 3 Binding motifs of the calcineurin’s binding partners.	9
Figure 4 A schematic diagram and sequence of CABIN1 fragments.....	28
Figure 5 Proline 2155 is essential for the interaction with calcineurin.....	29
Figure 6 Proline 2146 is critical for the interaction with calcineurin.....	30
Figure 7 CABIN1-L-1-2 (2146-2155) is the minimal peptide required to bind calcineurin.....	31
Figure 8 The “PPTP” sequence is important to interact with calcineurin.....	34
Figure 9 The role of the neighboring sequences around the “PxIxIT” motif.....	35
Figure 10 Protein stability of VIVIT peptides.....	36

Figure 11 The CABIN1 peptide inhibits NFAT transcriptional activity more efficiently than the VIVIT peptide.....	39
Figure 12 The CABIN1 peptide inhibits dephosphorylation of the NFATC2 more efficiently than the VIVIT peptide .....	40
Figure 13 The CABIN1 peptide inhibits nuclear import of the NFATC2 more efficiently than the VIVIT peptide .....	41
Figure 14 mRNA sequencing analysis upon T cell activation	44
Figure 15 Altered expression of the genes included in cluster III (1) .....	45
Figure 16 Altered expression of the genes included in cluster III (2) .....	46
Figure 17 The CABIN1 peptide binds to the same region of calcineurin as the VITIT peptide.....	49
Figure 18 The CABIN1 and VIVIT peptides do not affect the interaction between CNA and the “LxVP” motif .....	50
Figure 19 The interaction between CNA and the CABIN1 fragment is not affected by ionomycin treatment.....	51
Figure 20 The CABIN1 peptide does not inhibit calcineurin phosphatase activity .....	52

Figure 21 The “PPTP” sequence is critical for the interaction with calcineurin in the cellular level .....	55
Figure 22 Binding affinity of the substituted CABIN1 peptides for calcineurin (1) .....	56
Figure 23 Binding affinity of the substituted CABIN1 peptides for calcineurin (2) .....	57
Figure 24 No hydroxylation or O–GlcNAcylation occurred in the “PPTP” sequence .....	61
Figure 25 Binding affinity of threonine to valine substitutions of the CABIN1 peptide for calcineurin.....	62
Figure 26 TV substitution of the CABIN1 peptide restores the inhibitory effect on NFAT transcriptional activity .....	63
Figure 27 Phosphorylation of the threonine in “PPTP” is detected at the cellular level .....	64
Figure 28 Phosphorylation of CABIN1 T2154 enhances binding affinity for calcineurin .....	65
Figure 29 Screening of putative upstream kinases of the CABIN1 peptide upon PMA treatment.....	68
Figure 30 p38 MAPK phosphorylates 9th threonine of the CABIN1 peptide .....	69

Figure 31 p38 MAPK inhibitors reduce phosphorylation of the  
CABIN1 peptide and interaction with CNA..... 70

Figure 32 Putative calcineurin target genes that are not  
regulated via the calcineurin–NFAT pathway..... 78

# LIST OF ABBREVIATIONS

CABIN1	<i>C</i> -terminal fragment of calcineurin binding protein-1
CaM	Calmodulin
CNA	Calcineurin A
CNB	Calcineurin B
GAL4 DBD	GAL4 DNA binding domain
IL	Interleukin
NFAT	Nuclear factor of activated T cells
PMA	Phorbol myristate acetate
PTM	Post-translational modification
SPR	Surface plasma resonance
TCR	T cell receptor
VP16 AD	VP16 activation domain

# I . INTRODUCTION

## 1–1. The properties and roles of calcineurin

### 1–1–1 Domain organization and mechanism of activation

Calcineurin, a calcium and calmodulin–dependent serine/threonine phosphatase, is a heterodimer consisting of a catalytic A subunit (calcineurin A; CNA) and a regulatory B subunit (calcineurin B; CNB). CNA has a catalytic domain at the *N*–terminus and regulatory domains such as a CNB binding domain, a calmodulin (CaM) binding domain and two autoinhibitory domains at the *C*–terminus<sup>1,2</sup> (Figure 1a). The domain organization and catalytic domain sequences are well conserved across all eukaryotic species, but the *N*–terminal and *C*–terminal sequences are highly variable<sup>3</sup>. CNB harbors four highly conserved Ca<sup>2+</sup>–binding EF hands and a CNA binding site within the *C*–terminal EF hand<sup>2</sup> (Figure 1a). The *N*–terminal two EF hands have a relatively low binding affinity for Ca<sup>2+</sup>, whereas the *C*–terminal two EF hands have a relatively high binding affinity<sup>4</sup>.

According to the widely accepted model of calcineurin activation, calcineurin requires sequential conformational changes for full activation<sup>5,6</sup>. At steady state (low Ca<sup>2+</sup> levels), the autoinhibitory domain binds to the substrate–binding cleft and blocks the enzymatic activity. However, when the intracellular Ca<sup>2+</sup> levels

increase, the autoinhibitory domain is released from the active site depending on the conformational change of CNA induced by the interaction with calmodulin<sup>1</sup> (Figure 1b).

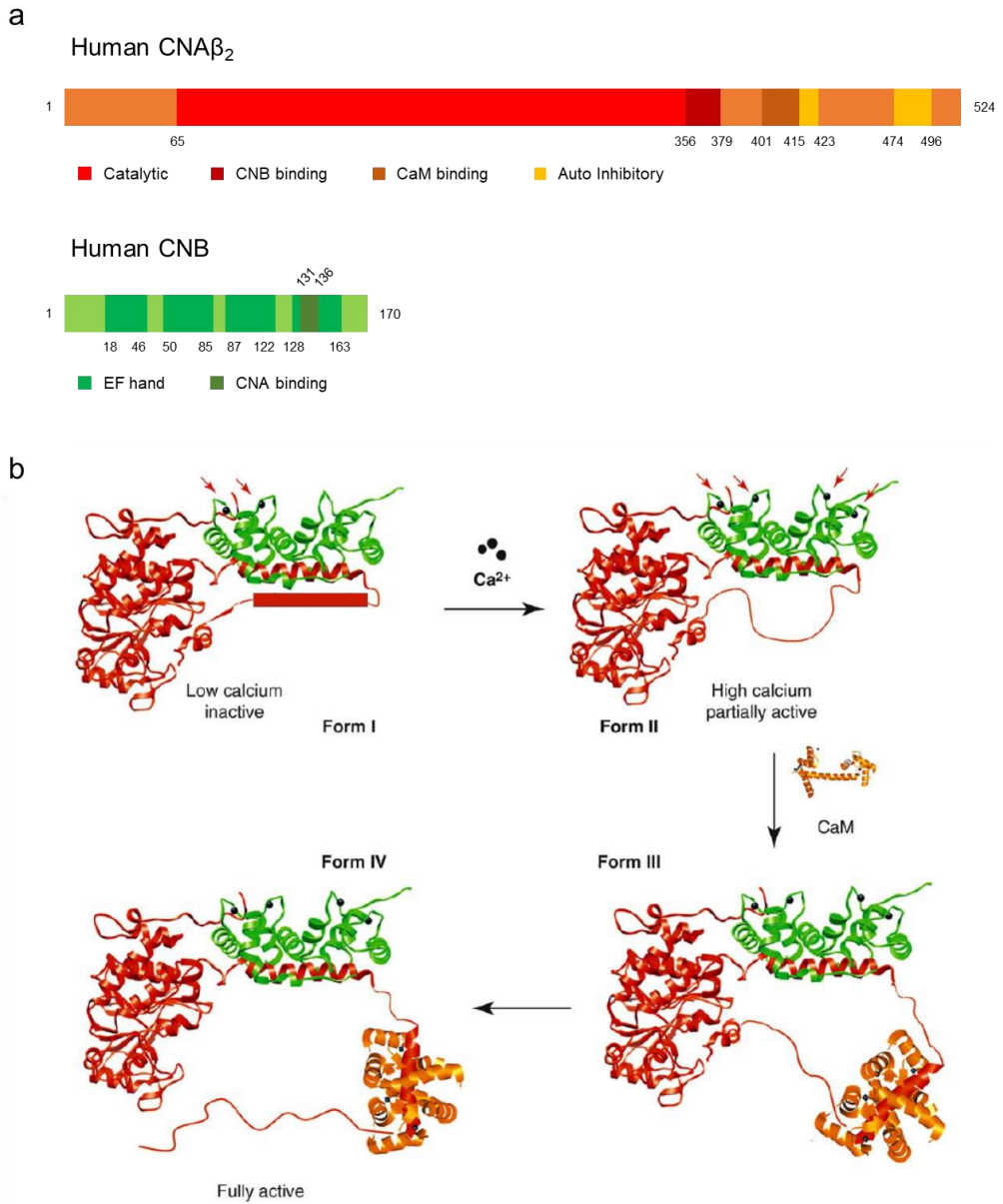


**Figure 1** Domain composition and mechanism of activation of calcineurin

**a** A schematic illustrate of calcineurin domain composition.

**b** A schematic model of calcineurin's sequential activation mechanism. CNA and CNB are shown in red and green, respectively. (Modified from Huiming Li et al., 2011)

## 1-1-2 The role of calcineurin in T cell activation

Calcineurin plays a pivotal role in diverse organs or cells, such as the brain, cardiovascular and skeletal muscle, pancreas  $\beta$  cells, and T lymphocytes<sup>7-10</sup>. Among them, the role related to T lymphocyte activation is best known. Productive activation of T lymphocytes requires T cell receptor (TCR) signaling and costimulatory signaling to act together. TCR signaling or costimulatory signaling alone leads to T cell anergy or tolerance<sup>11,12</sup>. TCR stimulation activates the calcineurin-NFAT pathway by elevating intracellular  $\text{Ca}^{2+}$  concentrations<sup>13</sup>, and simultaneous stimulation of TCR/CD28 activates the PKC-MAPK and PKC-IKK-NF $\kappa$ B pathways<sup>14,15</sup>. The calcineurin-NFAT and PKC-MAPK pathways activate NFAT and AP-1 (Fos/Jun), which cooperate in the transcriptional activation of proinflammatory cytokines, such as interleukin (IL)-2, -3, -4, GM-CSF, and IFN- $\gamma$ , thereby activating T lymphocytes<sup>16</sup> (Figure 2). However, PKC activation antagonizes the  $\text{Ca}^{2+}$ -induced calcineurin-NFAT pathway, despite being important for T lymphocyte activation<sup>17</sup>. PKC-activated p38 MAPK phosphorylates nuclear NFATC2 (also known as NFAT1 or NFATp), thereby exporting NFATC2 to the cytosol<sup>18</sup>.

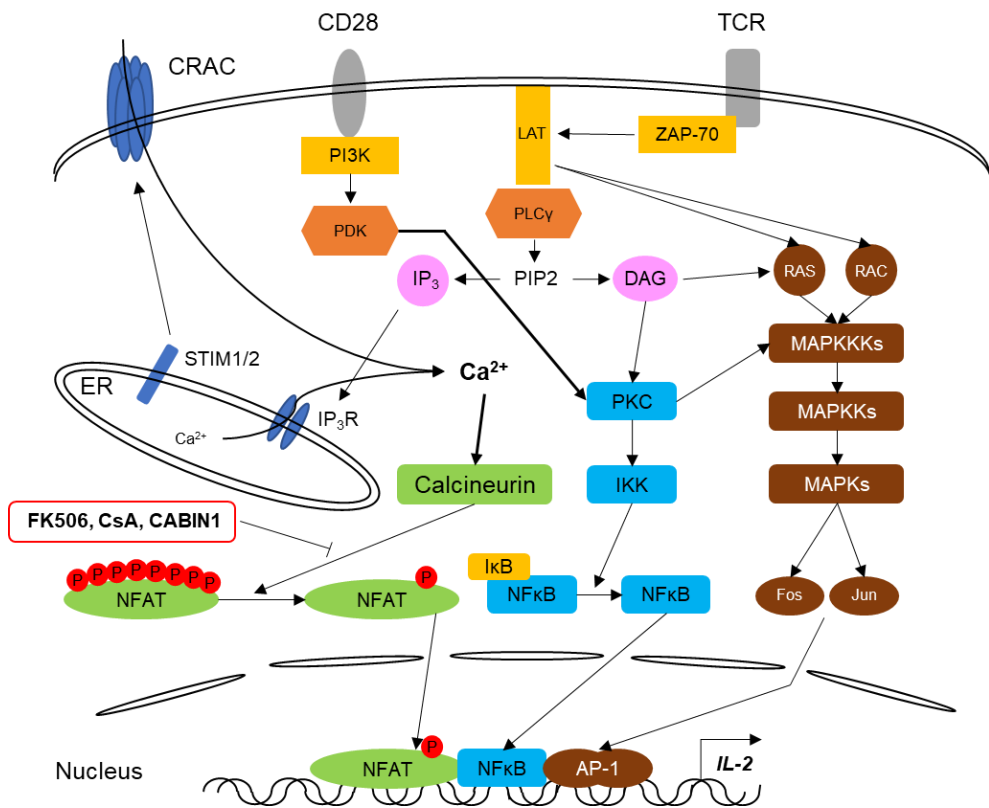


**Figure 2 Major T cell signaling pathways for activation**

A schematic diagram of T cell signaling pathways. Cooperation of the TCR with the costimulatory CD28 receptors promotes the productive activation of T cells. TCR signaling increases intracellular Ca<sup>2+</sup> levels and then activates the calcineurin–NFAT pathway (green). Engagement of TCR and CD28 signaling activates the PKC–IKK–NFκB pathways (blue) and the PKC–MAPK pathway (brown).

## 1–2. Substrates and inhibitors of calcineurin

Over the past few decades, many substrates and inhibitors of calcineurin containing conserved motifs for interaction with calcineurin, “PxIxIT” and/or “LxVP,” have been identified<sup>1,19,20</sup> (Figure 3a). For instance, the NFAT family members are well-known for calcineurin substrates containing both binding motifs<sup>1</sup>. In calcineurin-regulated NFATs (all NFAT family members except NFAT5), calcineurin dephosphorylated at least 13 conserved phosphorylation sites<sup>21</sup>. These sites are in the NFAT-homology region between the “PxIxIT” and “LxVP” motifs<sup>22</sup> (Figure 3b). Several kinases, such as GSK3, CK1, p38, and JNK, phosphorylate these sites. They cause conformational changes of NFAT, exposing nuclear export signals and masking nuclear localization signals<sup>23</sup>. Conventional calcineurin inhibitors, FK506 and cyclosporin A, respectively cooperating with FKBP12 or cyclophilin, bind to a hydrophobic pocket at the interface of CNA and CNB and compete with an LxVP-based peptide<sup>24</sup>. Furthermore, these immunosuppressant-immunophilin complexes spatially hinder the substrates’ access to the active site of calcineurin, inhibiting its phosphatase activity<sup>25,26</sup>. Thus, they cause serious side effects such as nephrotoxicity, fibrogenesis, neurotoxicity, and diabetes<sup>27</sup>.

However, they are still widely used in autoimmune diseases and organ transplant patients due to their convenient dosing and effectiveness<sup>27</sup>. Although several alternative calcineurin inhibitors have been developed over the past few decades, none have become clinical treatments so far. The VIVIT peptide, an optimized peptide derived from the conserved “PxIxIT” sequence of the NFAT family, blocks the interaction between calcineurin and NFAT without affecting calcineurin’s phosphatase activity<sup>28</sup>. Although it showed potential as an alternative calcineurin inhibitor for various calcineurin–NFAT pathway–dependent diseases, it has high IC<sub>50</sub> and drug delivery limitations<sup>19</sup>.

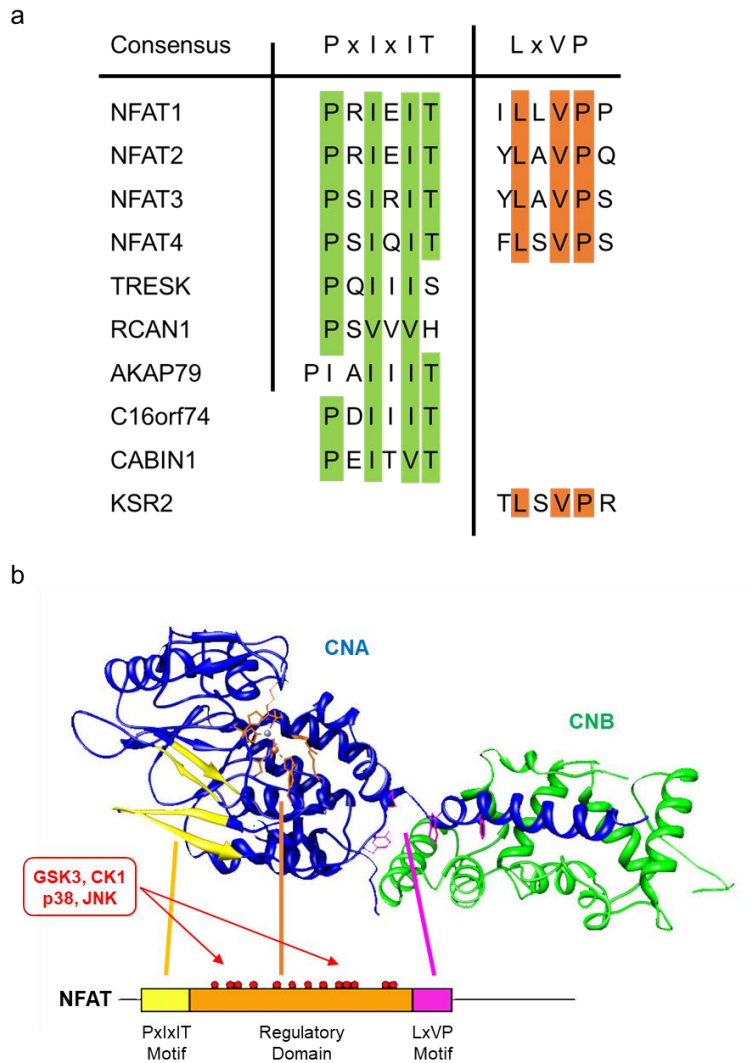


**Figure 3 Binding motifs of the calcineurin’s binding partners**

**a** Amino acid sequences belonging to two consensus calcineurin binding motifs of calcineurin’s binding partners.

**b** Interaction regions between calcineurin and NFAT. CNA and CNB are shown in blue and green, respectively. The “PxIxIT” motif of NFAT and its binding region on CNA are shown in yellow. The “LxVP” motif of NFAT and its binding site are shown in pink. The regulatory domain of NFAT and the active site of calcineurin are shown in orange. NFAT phosphorylation sites and its upstream kinases are shown in red. (Modified from Liu et al., 2009)

### 1–3. CABIN1, an endogenous calcineurin inhibitor

CABIN1 was first identified as an endogenous calcineurin inhibitor protein. Upon T cell activation, the CABIN1 C-terminal fragment binds to and inhibits calcineurin, thereby blocking NFAT dephosphorylation and repressing the *IL-2* promoter's transcriptional activation<sup>29</sup>. Although the C-terminus of CABIN1 contains a “PxIxIT” motif (Figure 3a), it is unknown whether this fragment's calcineurin inhibitory effect is due to the “PxIxIT” motif. Furthermore, the CABIN1 C-terminal fragment contains “PPTP” sequence instead of the “GPHEE” sequence of the VIVIT peptide following the “PxIxIT” motif. According to a research about structure of the calcineurin–VIVIT complex, the amino acid residues in the “GPHEE” sequence are less important for interaction with calcineurin<sup>30</sup>. However, the artificial peptidyl calcineurin inhibitor, ZIZIT–cisPro, shows better performance by modifying the proline in the “GPHEE” sequence<sup>31</sup>. Therefore, we need to determine the “PPTP” sequence contributes to the interaction with calcineurin. Finally, we need to identify a minimal and essential region that interact with calcineurin and the mechanism of the interaction for developing an alternative calcineurin inhibitor using CABIN1 C-terminal fragment.

## II. MATERIALS AND METHODS

## 2–1. Cell culture and transfection

HEK293T and Jurkat T (E6–1) cells were purchased from ATCC (Manassas, VA, USA). HEK293T cells were cultured in Dulbecco's modified Eagle's medium supplemented with 10% (v/v) fetal bovine serum (Gibco, Grand Island, NY, USA) and antibiotics at 37 °C and 5% CO<sub>2</sub> and transfected them using polyethyleneimine (Polysciences, Warrington, FL, USA). Jurkat T cells were cultured in RPMI 1640 medium supplemented with 10% (v/v) fetal bovine serum (Gibco), 2 mM L–glutamine (Gibco), and antibiotics at 37 °C and 5% CO<sub>2</sub>. Following the manufacturer's instructions, Jurkat T cells were transfected by electroporation using a Neon™ Transfection System (Thermo Fisher Scientific, Waltham, MA, USA).

## 2–2. Plasmid DNAs

Plasmid DNAs encoding calcineurin catalytic subunit (CNA) isoforms, CABIN1–14, CABIN1–15, tNFATC2, pG5–luc, and NFAT–luc were described previously<sup>29</sup>. The CNA isoforms were cloned into expression vectors such as pVP16, pRSET–A/B, and pCAG–Flag. Oligonucleotides of CABIN1, VIVIT, and chimeric and substituted peptides were obtained from Macrogen (Seoul, Korea)

or Cosmogenetech (Seoul, Korea). Each pair of complementary oligonucleotides was annealed for hybridization, and inserted into expression vectors such as pM, pGEX4T-1, pCAG-HA-GST, and pCAG-HA-mCherry. The pCAG-EGFP-tNFATC2-IRES-mCherry-peptide was constructed by replacing the puromycin resistance gene following the IRES segment with the mCherry-peptide. All the constructs were confirmed by sequencing.

## 2-3. Reagents and antibodies

The anti-GAL4 DNA binding domain (GAL4 DBD) (RK5C1) antibody was purchased from Santa Cruz Biotechnology (Dallas, TX, USA) and anti-NFATC2, pan-CNA, and phospho-MAPK Substrates Motif [PXpTP] antibodies were purchased from Cell Signaling (Danvers, MA, USA). Anti- $\beta$ -actin (AC-15) and Flag (M2) antibodies and Anti-FLAG @ M2 Affinity Gel were acquired from Sigma-Aldrich (St. Louis, MO, USA). The anti-HA (16B12) antibody was purchased from BioLegend (San Diego, CA, USA) and Pierce™ Anti-HA Agarose was purchased from Thermo Fisher Scientific. Phorbol myristate acetate (PMA) and ionomycin were obtained from Sigma-Aldrich, FK506 was obtained from InvivoGen (San Diego, CA, USA), and EO 1428 and TAK 715 were obtained from Tocris (Bristol, UK).

## 2-4. Peptide synthesis

The unlabeled peptides (CABIN1-L-1 [MAGFPPEITVTPPTP] and VIVIT 15-mer [MAGPHPVIVITGPHEE]) were synthesized by Pepton (Daejeon, Korea). The biotin-labeled peptides (VEET [Biotin-AAAMAGPPHIVEETGPHVI], VIVIT 15-mer [Biotin-AAAMAGPHPVIVITGPHEE], CABIN1-L-1 [Biotin-AAAMAGFPPEITVTPPTP], and phosphorylated CABIN1-L-1 [Biotin-AAAMAGFPPEITVTPP{pTHR}P]) were synthesized by GenScript (Piscataway, NJ, USA). All the peptides were purified by HPLC and were >95% pure, and their molecular weight and composition were analyzed by mass spectrometry.

## 2-5. Luciferase reporter assay

To measure the transcriptional activity of NFAT, Jurkat T cells were cotransfected with GST-tagged peptides and NFAT-luc by electroporation. After 24 h, the cells were pretreated with 0.5  $\mu$ M FK506 for 1 h and then treated with 40 nM PMA and 1  $\mu$ M ionomycin for 8 h. For the mammalian two-hybrid assay, HEK293T cells were cotransfected with GAL4 DBD-tagged CABIN1, VIVIT, chimeric and substituted peptides, VP16 activation domain (VP16

AD)-tagged CNA $\beta_2$ , and pG5-luc (luciferase reporter plasmid containing the GAL4-responsive promoter) for 24 h. The harvested cells were lysed with a luciferase assay lysis buffer (17 mM KH<sub>2</sub>PO<sub>4</sub>, 183 mM K<sub>2</sub>HPO<sub>4</sub>, pH 7.8, 0.2% [v/v] Triton X-100) and sonicated briefly. Luciferase activity was measured for each cell lysate using an Infinite M200 (Tecan, Männedorf, Switzerland). In addition, the expression level of the transfected proteins was confirmed by western blotting.

## **2-6. Immunoprecipitation assay**

Cells were lysed in IP150 buffer (25 mM Tris-HCl, pH 8.0, 150 mM NaCl, 1 mM EDTA, pH 8.0, 0.1% [v/v] NP-40, 10% [v/v] glycerol and protease inhibitor cocktail) for 30 min on ice and cell lysates were harvested by centrifugation at 15000 rpm for 10 min. Flag- and HA-tagged proteins were immunoprecipitated with Anti-FLAG ® M2 Affinity Gel (Sigma-Aldrich) and Pierce™ Anti-HA Agarose (Thermo Fisher Scientific), respectively, for 2 h at 4 °C. Beads were washed three times with IP150 buffer and captured proteins were eluted with 2.5X sample buffer, separated by SDS-PAGE, transferred to NC membrane and immunoblotted with indicated antibodies . To quantify the western blot results, the band areas were measured using ImageJ (<https://imagej.nih.gov/ij/>).

## 2–7. Protein purification and in vitro binding assay

GST-tagged peptides and His-tagged CNA $\alpha$  and  $\beta_2$  were expressed and purified in *Escherichia coli* BL21 (DE3)pLysS. When the optical density (OD 600 nm) reached 0.5, IPTG was treated to the bacteria (0.1 mM overnight at 18 °C or 1 mM for 4 h at 37 °C). Cells were harvested by centrifugation at 5000 rpm for 10 min and resuspended in bacteria lysis buffer (20 mM Tris-HCl, pH 8.0, 137 mM NaCl, 1.5 mM MgCl<sub>2</sub>, 10% [v/v] glycerol, 0.2 mM PMSF and protease inhibitor cocktail). Resuspended cells were sonicated and added 1% (v/v) Triton X-100. Insoluble materials were pelleted by centrifugation at 15000 rpm for 15 min. The supernatant was mixed with pre-equilibrated Glutathione Sepharose™ 4 Fast Flow (Cytiva, Marlborough, MA, USA) or Ni-NTA agarose beads (QIAGEN, Hilden, Germany) for 1 h at 4 °C with gentle rotation. Beads were washed with 1% (v/v) TritonX-100 contained bacteria lysis buffer three times and eluted with elution buffer (100 mM Tris-HCl, pH 8.0, 150 mM NaCl, 10% [v/v] glycerol and 10 mM reduced glutathione for GST-tagged proteins or 500 mM imidazole for His-tagged proteins) for 1 h at 4 °C with gentle rotation. Eluted proteins were concentrated using 10 kDa Amicon centricon devices. The

concentration of purified protein was analyzed by Coomassie Brilliant Blue staining of SDS-PAGE gel. His-pull down assay was performed with 0.5 ml of IP150 buffer with 0.5 mM EDTA. His-tagged CNA was mixed with GST-tagged peptides and immobilized on Ni-NTA agarose beads. The beads were washed three times with binding buffer and analyzed the proteins by western blotting. GST-tagged peptides were pulled down using Glutathione Sepharose™ 4 Fast Flow and biotin-labeled peptides were pulled down using Streptavidin Agarose Resin (Thermo Fisher Scientific).

## **2-8. In vitro kinase assay**

The purified GST-tagged peptides were used for the in vitro kinase assays with activated recombinant kinases obtained from Proqinase GmbH (Freiburg, Germany). Kinase assays were performed in reaction buffer (50 mM HEPES-NaOH, pH 7.5, 3 mM MgCl<sub>2</sub>, 3 mM MnCl<sub>2</sub>, 3 μM sodium orthovanadate, 1 mM dithiothreitol, 50 μM unlabeled ATP, 5 μCi <sup>32</sup>P-γ-ATP) for 1 h at 30 °C. The reaction was stopped by adding 5X sample buffer and the proteins were separated using SDS-PAGE. The gel was stained with Coomassie Brilliant Blue, dried, and developed on X-ray film.

## 2–9. Confocal microscopy and analysis

Jurkat T cells were transfected with the pCAG–EGFP–tNFATC2–IRES–mCherry–peptide by electroporation. After two days, these cells were pretreated with 0.5  $\mu$ M FK506 for 30 min, and then treated with 40 nM PMA and 1  $\mu$ M ionomycin under culture conditions for 4 h. Before imaging by a confocal laser scanning microscope (Nikon, Tokyo, Japan), nuclei of the cells were stained with 10  $\mu$ g/ml Hoechst 33342 (Invitrogen, Waltham, MA, USA). Colocalization analysis of mCherry and Hoechst was performed with ImageJ and its plugin JACoP to measure the Manders coefficient<sup>32,33</sup>.

## 2–10. Calcineurin activity assay

Calcineurin phosphatase activity was measured in vitro using a calcineurin phosphatase assay kit (BML–AK804, Enzo Life Sciences, Farmingdale, NY, USA). GST or GST–tagged peptides were incubated with CNA for 30 min at room temperature, then subsequent steps followed the manufacturer’s instructions. To measure endogenous calcineurin phosphatase activity, Jurkat T cells were transiently transfected with CAG–HA–mCherry–peptides by electroporation. After 24 h, the Jurkat T cells were pretreated with FK506 for 1 h and then activated with PMA and

ionomycin. Next, the cells were washed with TBS buffer (20 mM Tris-HCl, pH 7.2, 150 mM NaCl), resuspended with lysis buffer from the calcineurin cellular activity assay kit (BML-AK816, Enzo Life Sciences), and kept on ice for 30 min. The lysate supernatant was collected and removed free phosphate by gel filtration using the Desalting Column Resin included in the kit. Then, subsequent steps followed the manufacturer's instructions.

## 2-11. Real-time quantitative PCR

Jurkat T cells were harvested and lysed with QIAzol Lysis Reagent (Qiagen) to extract total RNA. cDNAs were synthesized via reverse transcription from isolated RNA using AMV Reverse Transcriptase and random hexamers. Real-time quantitative PCR was performed on each cDNA using TB Green® Premix Ex Taq™ (TaKaRa, Kusatsu, Japan) on a CFX Connect Real-time PCR Detection System (Bio-Rad, Hercules, CA, USA). The results were normalized to that of *18S rRNA* or *GAPDH*.

Real-time qPCR primer for *IL-2*

5'-ACAGCTACAACCTGGAGCATTTA-3'

5'-TCAGTTCTGTGGCCTTCTTG-3'

Real-time qPCR primer for *IL-3*

5'-GCTGGACTTCAACAACCT-3'

5'-CAGACATGGCAGGAGATTT -3'

Real-time qPCR primer for *CCL4*

5'-GTACGTGTATGACCTGGAAC-3'

5'-GAGATGTGTCTCATGGAGAAG-3'

Real-time qPCR primer for *CCL20*

5'-GACTGCTGTCTTGGATACAC-3'

5'-TACTGAGGAGACGCACAA-3'

Real-time qPCR primer for *CXCL8*

5'-GAACCATCTCACTGTGTGTAA-3'

5'-TGGAAAGGTTTGGAGTATGTC-3'

Real-time qPCR primer for *NFATC1*

5'-CCGTTACGTCAGTTTCTAC-3'

5'-GTTGGAGCAGGCTCATAATC-3'

Real-time qPCR primer for *CD27*

5'-GCACTGTA ACTCTGGTCTTC-3'

5'-GGGTTTGG AAGAGGATCAC-3'

Real-time qPCR primer for *CD70*

5'-GATGGCATCTACATGGTACAC-3'

5'-GGTACAACCTTGGTGG AAG-3'

Real-time qPCR primer for *NINJ1*

5'-CCTCATCTCCATCTCCCTT-3'

5'-GTTGACTACCACGATGATGAA-3'

Real-time qPCR primer for *ZP4*

5'-GGAGACCGAGCAGTATATGA-3'

5'-CTGGACATTGATTGGGAGAG-3'

Real-time qPCR primer for *mCherry*

5'-ACGGCGAGTTCATCTACA-3'

5'-TCAGCCTCTGCTTGATCT-3'

Real-time qPCR primer for *18S rRNA*

5'-GCTTAATTTGACTCAACACGGGA-3'

5'-AGCTATCAATCTGTCAATCCTGTC-3'

Real-time qPCR primer for *GAPDH*

5'-CCGTCTAGAAAAACCTGCC-3'

5'-GCCAAATTCGTTGTCATACC-3'

## 2-12. mRNA sequencing and analysis

Jurkat T cells expressing HA-mCherry-peptides were pretreated with FK506 for 1 h and then activated with PMA and ionomycin for 8 h. Then, RNAs were extracted from these cells. Construction of the cDNA library and next-generation sequencing were performed

at LAS (Gimpo, Korea). All samples were sequenced on an Illumina NextSeq 500 system with 75 paired-end reads. For the RNA sequencing analysis, reads for each sample were aligned to the human genome (GRCh37/hg19 genome assembly) using STAR 2.4.0.1<sup>34</sup> with default settings. HOMER tools were used to quantify and normalize the defined genes in RefSeq transcripts. FPKM normalized genes were hierarchically clustered using Cluster3.0<sup>35</sup>. Refined data was visualized with Java Treeview (<http://jtreeview.sourceforge.net>). Gene ontology analysis of each cluster was conducted using the DAVID web tool (<https://david.ncifcrf.gov>). Finally, the expression levels of target genes were visualized using the Integrative Genomics Viewer (<http://software.broadinstitute.org/software/igv>). The raw data were submitted to the NCBI Gene Expression Omnibus under accession number GSE185561.

## **2–13. Flow cytometry**

The expression of mCherry-tagged VIVIT peptides was quantified using LSRII (SORP) (Becton Dickinson, Franklin Lakes, NJ, USA). The results were analyzed with FlowJo (Tree Star, Inc., Ashland, OR, USA).

## 2-14. Mass spectrometry

The protein HA-mCherry-CABIN1-L-1-2 expressed in Jurkat T cells was purified by immunoprecipitation of 4 mg lysates with Pierce™ Anti-HA Agarose. The bead-bound proteins were eluted by competition with 1 mg/ml HA peptide. After separation by SDS-PAGE and staining with Coomassie Brilliant Blue, LC-MS/MS was performed to analyze the purified proteins by ProteomeTech (Seoul, Korea).

## 2-15. Surface plasmon resonance

Using a Biacore T200 (Cytiva), the biotin-labeled peptides were captured on the surface of a Series S Sensor Chip SA (Cytiva). Purified His-tagged CNA was serially diluted in HBS-EP+ (10 mM HEPES, pH 7.4, 150 mM NaCl, 3 mM EDTA, 0.05% surfactant P20) and passed sequentially over three flow cells (flow cell 1: biotin-VEET, flow cell 2: biotin-CABIN1-L-1, flow cell 3: biotin-p-CABIN1-L-1). Each cycle was performed at 25 °C at a flow rate of 30 µl/min with 120 s of contact and 240 s of dissociation. The kinetics of interactions was analyzed using BIAevaluation 3.2 RC1 (Cytiva).

## 2–16. Statistics

All data are presented as the mean  $\pm$  standard deviation from at least three biologically independent trials. P values were calculated using a two-tailed Mann–Whitney U test to compare two groups. The Kruskal–Wallis Test was used to analyze multiple groups. The p values  $< 0.05$ ,  $< 0.01$ , and  $< 0.001$  appear as single, double, and triple asterisks, respectively. NS indicates a nonsignificant difference ( $p \geq 0.05$ ).

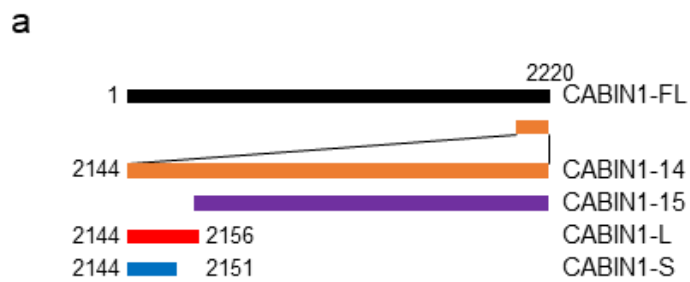
### III. RESULTS

### **3-1. The 10 amino acids of CABIN1 (2146-2155) are essential for the interaction with calcineurin**

To determine the minimal sequence binding to calcineurin, we separated the first 13-amino acid segment containing the “PxIxIT” motif (named CABIN1-L) from CABIN1-14 (Figure 4a, b). We performed a mammalian two-hybrid assay using the GAL4 DBD-tagged CABIN1 peptides and VP16 AD-tagged CNA (Figure 5). The results confirmed that CABIN1-14 binds to CNA as previously reported<sup>29</sup>, while the other sequences (CABIN1-15) did not.

We designed several peptides by sequentially removing the CABIN1-L C-terminal amino acid residues (Figure 4b; CABIN1-S ~ CABIN1-L). The mammalian two-hybrid interaction assay showed that CABIN1-L and CABIN1-L-1 had a stronger affinity for CNA than CABIN1-14 had. However, CABIN1-L-2 completely lost its binding affinity to CNA despite its higher expression level (Figure 5). Next, we designed additional peptides by sequentially removing the CABIN1-L-1 N-terminal amino acid residues (Figure 4b; CABIN1-L-1-1 ~ CABIN1-L-1-4). CABIN1-L-1-1 and CABIN1-L-1-2 are still bound to CNA, but CABIN1-L-1-3 lost its binding affinity (Figure 6). The immunoprecipitation assays using GAL4 DBD-tagged CABIN1 peptide and Flag-tagged

CNA showed identical results (Figure 7a, b). These results demonstrate that the 10 amino acids from proline 2146 to proline 2155 of full-length CABIN1 form the minimal sequence interacting with calcineurin.



**b**

Label	Sequence
CABIN1-S	FPPEITVT
CABIN1-L-4	FPPEITVTP
CABIN1-L-3	FPPEITVTPP
CABIN1-L-2	FPPEITVTPPT
CABIN1-L-1	FPPEITVTPPTP
CABIN1-L	FPPEITVTPPTPT
CABIN1-L-1-1	PPEITVTPPTP
CABIN1-L-1-2	PEITVTPPTP
CABIN1-L-1-3	EITVTPPTP
CABIN1-L-1-4	ITVTPPTP

**Figure 4** A schematic diagram and sequence of CABIN1 fragments

**a** A schematic diagram of CABIN1 full length and C-terminal fragments.

**b** Amino acid sequence of CABIN1 C-terminal fragments.

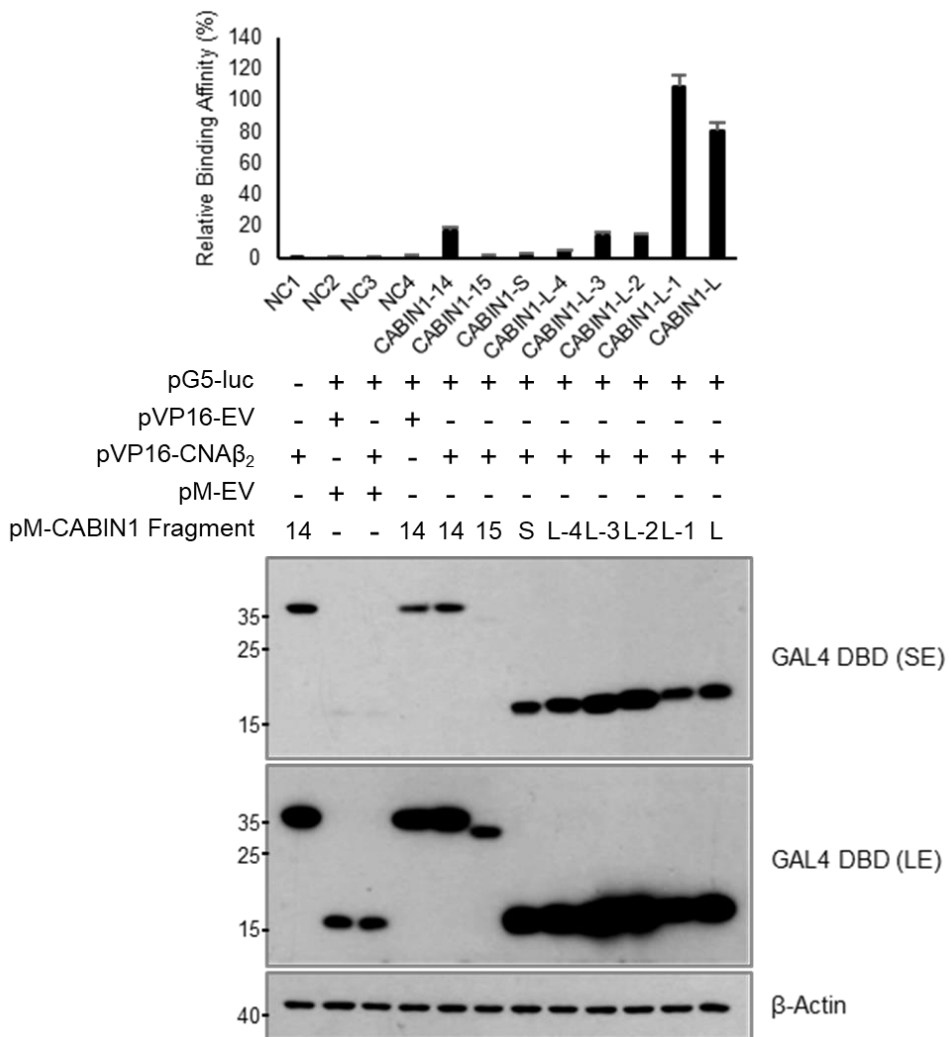


**Figure 5 Proline 2155 is essential for the interaction with calcineurin**

Mammalian two-hybrid assay was performed using VP16 AD-CNAβ<sub>2</sub> and GAL4 DBD-CABIN1 peptides (CABIN1-14, -15, -S ~ L) in HEK293T cells. SE, short exposure, LE, long exposure, NC, negative control, EV, empty vector.

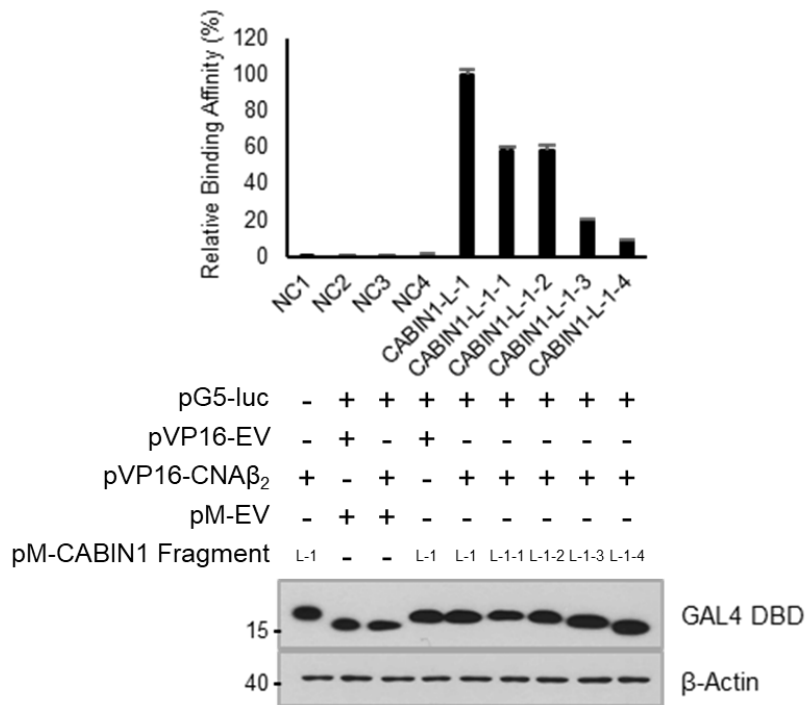


**Figure 6 Proline 2146 is critical for the interaction with calcineurin**

Mammalian two-hybrid assay was performed using VP16 AD-CNAβ<sub>2</sub> and GAL4 DBD-CABIN1 peptides (CABIN1-L-1 ~ L-1-4) in HEK293T cells. NC, negative control, EV, empty vector.

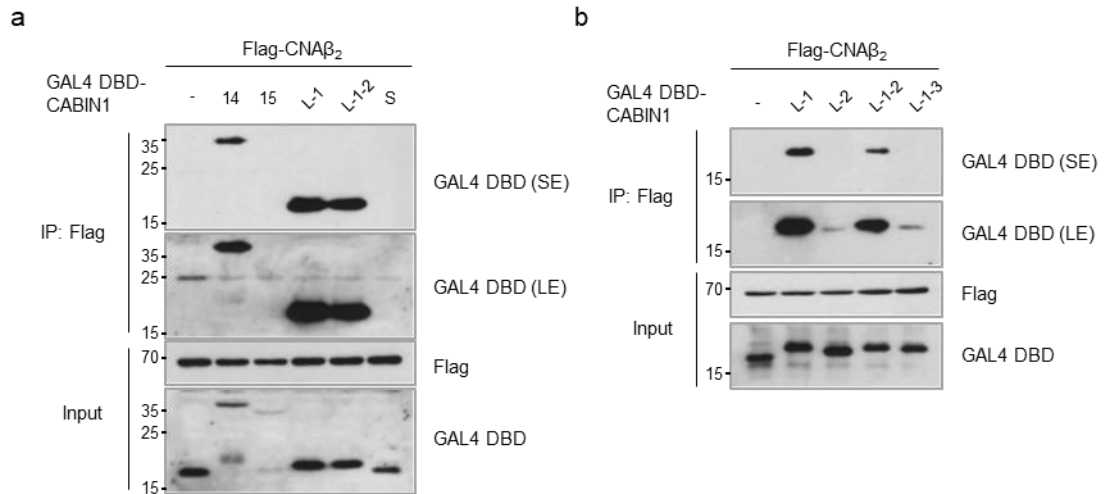


**Figure 7** CABIN1-L-1-2 (2146–2155) is the minimal peptide required to bind calcineurin

**a, b** HEK293T cells were transfected with Flag-CNA $\beta_2$  and GAL4 DBD-CABIN1 fragments, and immunoprecipitated with Flag antibody. The interaction between CNA $\beta_2$  and each CABIN1 fragment was detected with indicated antibodies. SE, short exposure, LE, long exposure.

### 3-2. The “PPTP” sequence following the “PxIxIT” motif is critical for the interaction with calcineurin

Previous research demonstrated the biochemical and structural significance of the “PxIxIT” motif<sup>28,30</sup>, but the role of the neighboring sequences around the “PxIxIT” motif in calcineurin binding remains unclear. Since proline 2155 does not belong to the “PxIxIT” motif, we needed to clarify the role of the *C*-terminal “PPTP” sequence following the “PxIxIT” motif. To compare the CABIN1 and VIVIT peptides under the same conditions, we used the VIVIT decamer (VIVIT 10-mer) as a control. We constructed a chimeric peptide by swapping the *C*-terminal sequences of the VIVIT and CABIN1 peptides and conducted a mammalian two-hybrid assay (Figure 8a, b). The *C*-terminal “PPTP” sequence enhanced the interaction with CNA by 4.76-fold (VIVIT PPTP vs. VIVIT 10-mer), while the *N*-terminal “PVIVIT” enhanced it by 1.93-fold (VIVIT PPTP vs. L-1-2 WT). This result suggests that the *C*-terminal “PPTP” sequence also plays an important role in the interaction with calcineurin.

Next, we checked whether the *N*-terminal sequence in front of the “PxIxIT” (“AGPH” in the VIVIT peptide and “FP” in CABIN1-L-1) contributed to the interaction with calcineurin. Adding “AG,” “PH,”

or “FP” before the “PxIxIT” motif did not affect the interaction with calcineurin (Figure 9a, b). Besides, these sequences did not affect the inhibitory effect of the calcineurin–NFAT pathway (Figure 9c). In the case of the VIVIT peptide, the *C*-terminal glutamate repeats decreased protein stability (Figure 10a–d).

a

Label	Sequence
VIVIT 10-mer	PVIVITGPHE
VIVIT PPTP	PVIVITPPTP
L-1-2 WT	PEITVTPPTP
L-1-2 GPHE	PEITVTGPHE

b

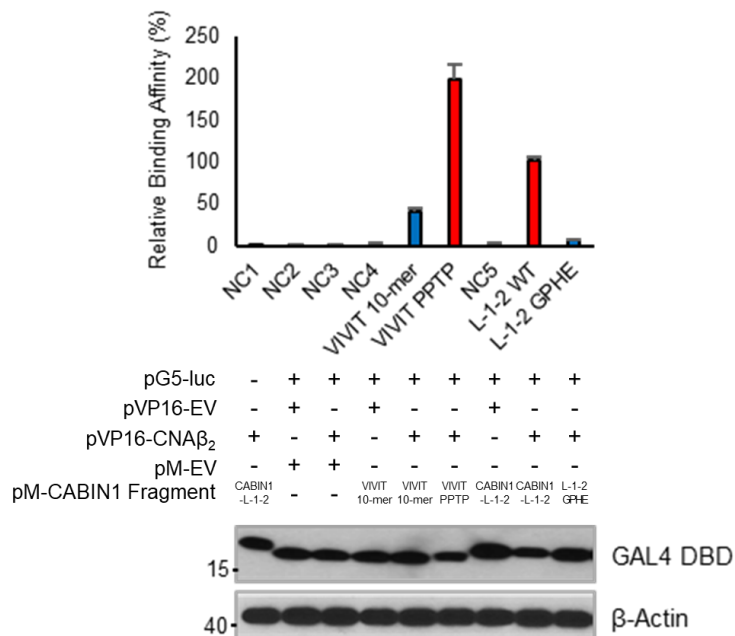


**Figure 8** The “PPTP” sequence is important to interact with calcineurin

**a** Amino acid sequence of CABIN1–L–1–2, VIVIT 10–mer and chimeric peptide. **b** Mammalian two–hybrid assay was performed using VP16 AD–tagged CNA $\beta_2$  and GAL4 DBD–tagged indicated peptide. NC, negative control, EV, empty vector.

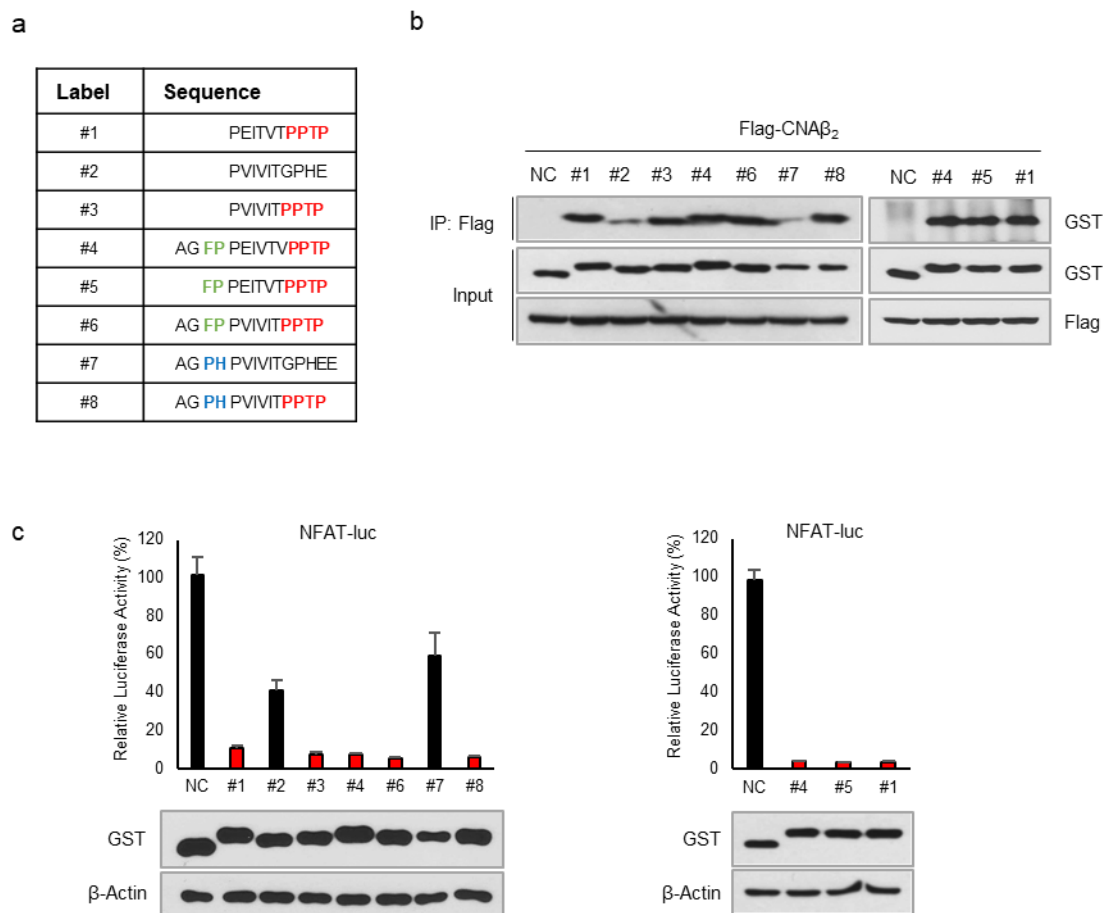


**Figure 9** The role of the neighboring sequences around the “PxIxIT” motif

**a** Amino acid sequence of CABIN1, VIVIT, and chimeric peptides.

**b** Immunoprecipitation assays using Flag–CNA $\beta_2$  and GST–peptides in

HEK293T. **c** Luciferase reporter assays were performed to measure

NFAT transcriptional activity in Jurkat T cells expressing GST–peptides

under PMA and Ionomycin treatment. NC, negative control.

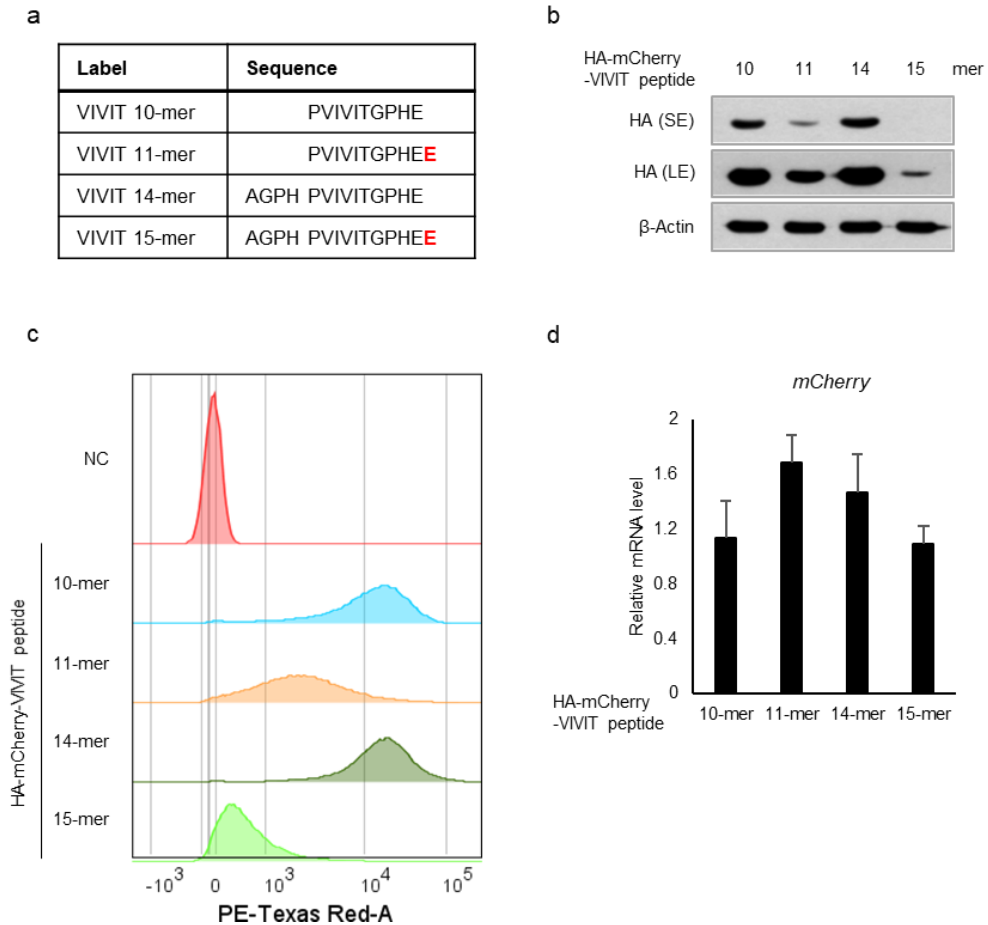


**Figure 10 Protein stability of VIVIT peptides**

**a** Amino acid sequence of VIVIT peptides. **b** Protein expression levels of VIVIT peptides were detected with HA antibody in Jurkat T cells expressing HA-mCherry-VIVIT peptides. **c** mCherry expression intensity and distribution were analyzed by FACS in the Jurkat T cells expressing HA-mCherry-VIVIT peptides. ( $5 \times 10^4$  cells/sample) **d** mRNA expression level of mCherry was measured by qRT-PCR. SE, short exposure, LE, long exposure, NC, negative control.

### **3-3. The CABIN1 peptide is a stronger Calcineurin-NFAT pathway inhibitor than the VIVIT peptide**

To investigate the inhibitory effect of the CABIN1 peptide on the calcineurin-NFAT pathway, we co-transfected the GST-tagged CABIN1-L-1-2 or VIVIT peptide into Jurkat T cells with a luciferase reporter gene under the control of three repeated NFAT binding sites. Upon treatment with PMA and ionomycin, expression of the GST-tagged CABIN1-L-1-2 or VIVIT peptide repressed luciferase activity compared with the negative control. The inhibitory effect of the CABIN1-L-1-2 was about four times stronger than that of the VIVIT peptide (Figure 11). To confirm that this result is due to NFATC2 dephosphorylation by calcineurin, we performed an NFAT mobility shifting assay. In T cells, NFATC1 and NFATC2 are hyperphosphorylated, and calcineurin dephosphorylates them in response to calcium signaling<sup>23</sup>. Hyperphosphorylated NFATs are localized in the cytosol, whereas dephosphorylated proteins are localized in the nucleus and migrate faster in gels than hyperphosphorylated proteins do<sup>36</sup>. Like FK506, the CABIN1 peptide significantly inhibited the NFATC2 band shift upon treatment with PMA and ionomycin (Figure 12a). The VIVIT peptide also reduced the dephosphorylation of NFATC2, but its

inhibitory effect was weaker than that of the CABIN1 peptide (Figure 12a, b).

Next, we constructed plasmids expressing EGFP-tagged truncated NFATC2 (tNFATC2; 2-460 amino acids) and mCherry-tagged each peptide at once to confirm these peptides' contribution to the NFAT nuclear import. The proportion of nuclear-localized tNFATC2 was lowest in FK506-treated cells and slightly higher in Jurkat T cells co-expressing the CABIN1-L-1-2 peptide. Meanwhile, Jurkat T cells co-expressing the VIVIT peptide showed a significantly higher proportion of nuclear-localized tNFATC2 than cells co-expressing the CABIN1-L-1-2 peptide (Figure 13a, b). Altogether, these results demonstrate that the CABIN1 peptide blocks the dephosphorylation and nuclear translocation of NFATC2 more efficiently than the VIVIT peptide does.

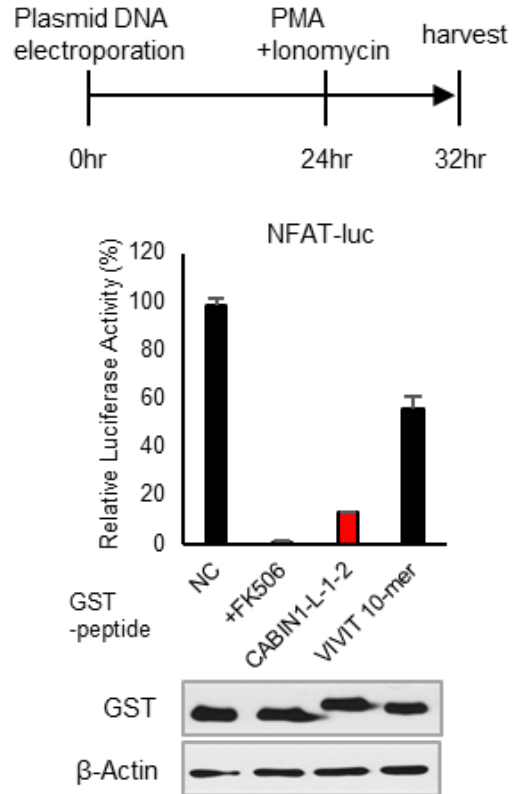


**Figure 11 The CABIN1 peptide inhibits NFAT transcriptional activity more efficiently than the VIVIT peptide**

Luciferase reporter assay was performed to measure NFAT transcriptional activity. Jurkat T cells expressing GST-peptides were treated with PMA and Ionomycin for activation. Jurkat T cells expressing GST were used as negative control, and cells treated with 0.5  $\mu$ M FK506 were used as a positive control. (n=3)

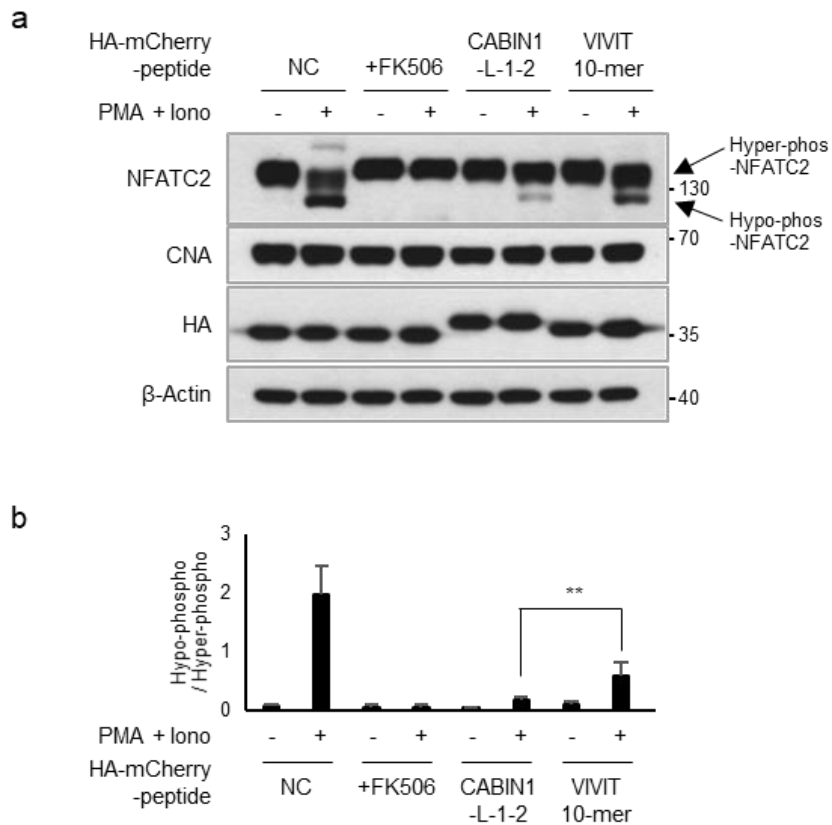


**Figure 12** The CABIN1 peptide inhibits dephosphorylation of the NFATC2 more efficiently than the VIVIT peptide

**a** NFAT mobility shifting assay was performed using Jurkat T cells expressing HA-mCherry-peptides. To induce dephosphorylation of NFATC2, Jurkat T cells were treated with PMA and ionomycin for 2 h.

**b** Hyper- and hypo-phosphorylated NFATC2 of **a** were measured using imageJ and the hypo/hyper-ratio was calculated. (n=7)

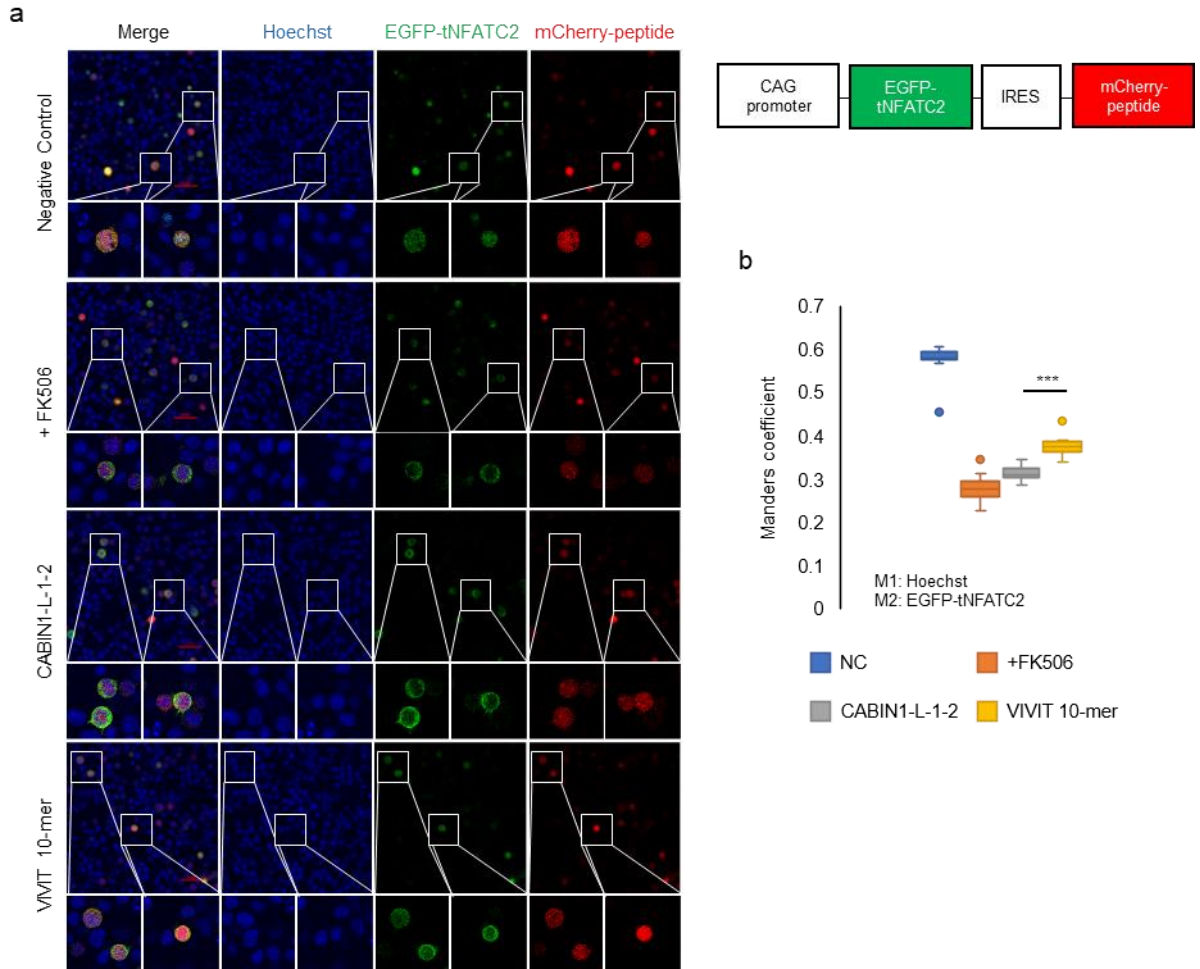


**Figure 13** The CABIN1 peptide inhibits nuclear import of NFATC2 more efficiently than the VIVIT peptide

**a** Snapshot images of activated Jurkat T cells expressing indicated peptides and tNFATC2 were obtained using confocal microscopy. Expression and localization of peptides and tNFATC2 were shown as mCherry (red) and EGFP (green), respectively. Nuclei were stained with Hoechst (blue). Scale bar, 50  $\mu$ m. **b** Nuclear localized tNFATC2 was measured by calculating the colocalization ratio between Hoechst (M1) and EGFP (M2). (NC and FK506, n=10, CABIN1-L-1-2 and VIVIT 10-mer, n=12) NC, negative control.

### 3–4. The CABIN1 peptide blocks T lymphocyte activation

To confirm whether the CABIN1 peptide blocks T lymphocyte activation by interfering with the calcineurin–NFAT interaction, we sequenced the RNA of Jurkat T cell lines stably expressing the negative control (mCherry only) and mCherry–tagged CABIN1 peptide. We found 685 genes affected by PMA and ionomycin treatment in negative control cells (Figure 14a). We focused on cluster III of four clusters, which contained genes with increased expression levels in the negative control group upon treatment with PMA and ionomycin, and reduced expression levels in CABIN1 peptide–expressing cells and FK506–treated cells. The gene ontology analysis revealed that the genes in cluster III are related to chemokines, cytokines signaling, and the immune response (Figure 14b). Furthermore, upon T cell activation, the CABIN1 peptide, and FK506 reduced the RNA levels of representative T cell activation markers, such as *IL2*, *IL3*, *NFATC1*, and various chemokine ligands (*CCL4*, *CCL20*, *CXCL8*). Besides, the CABIN1 peptide and FK506 also repressed *CD27* and *CD70*, which regulate the T cell costimulatory pathway (Figure 15). The real–time quantitative PCR analysis of these genes showed that the CABIN1

peptide reduced the RNA levels of these genes more efficiently than the VIVIT peptide did (Figure 16).

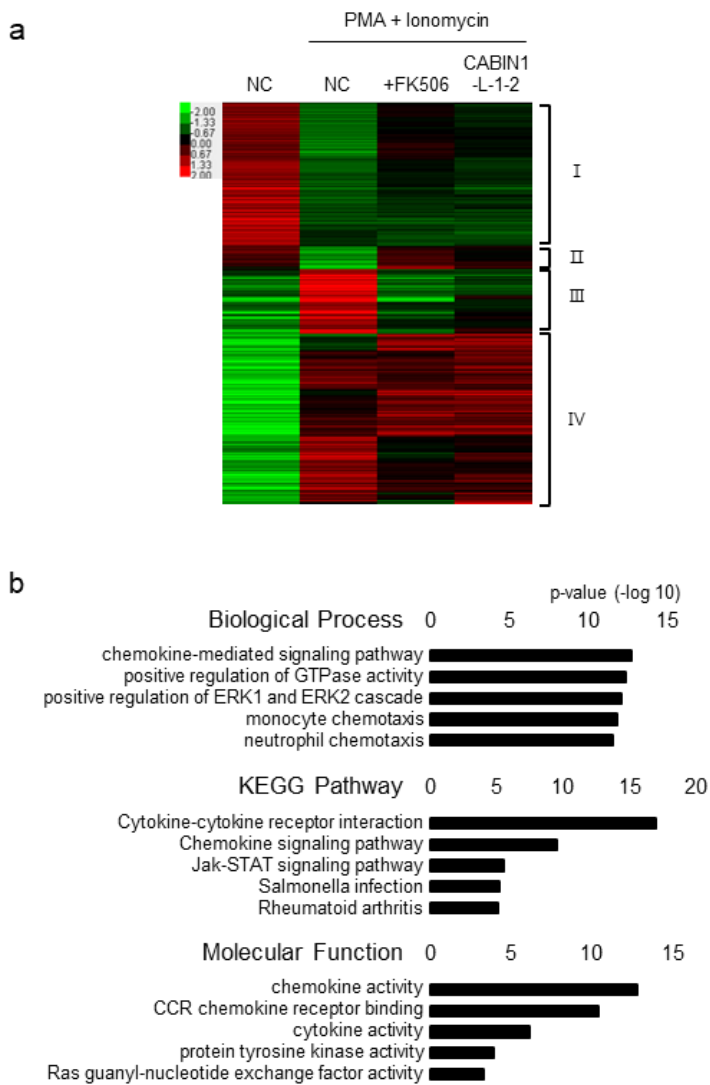


**Figure 14 mRNA sequencing analysis upon T cell activation**

**a** Heat map of altered genes affected by FK506 treatment or CABIN1 peptide expression upon T cell activation.

**b** The gene ontology analysis of cluster III.

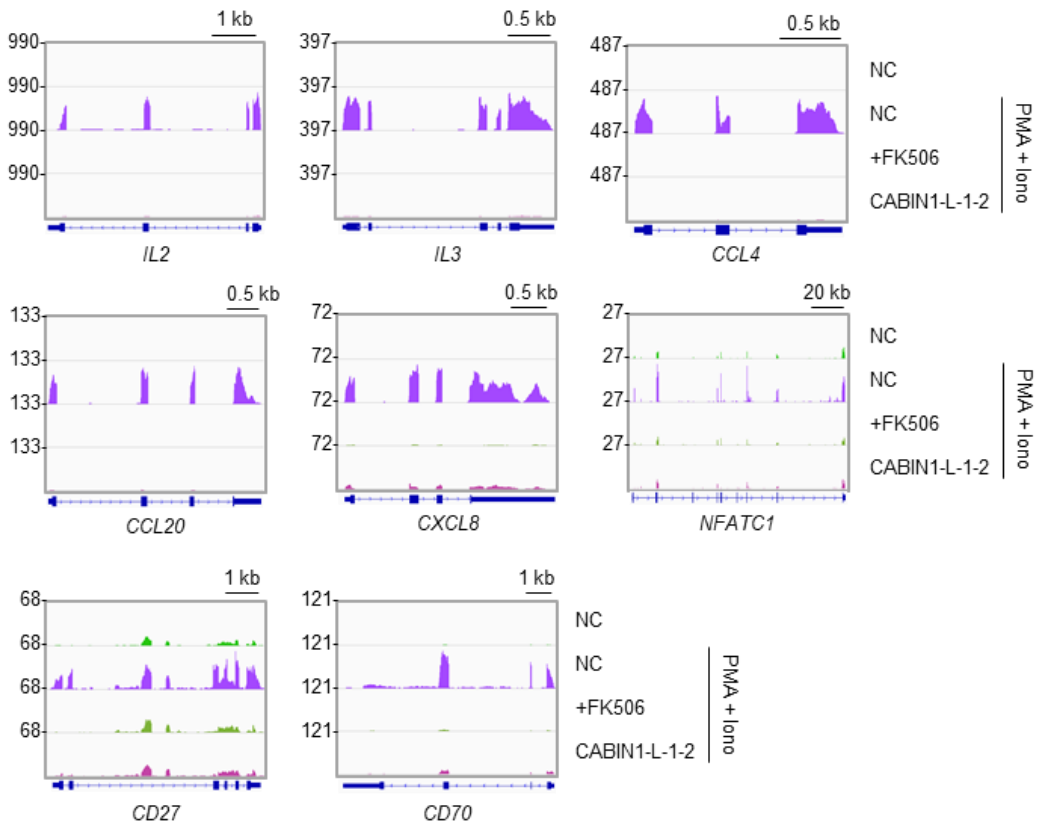


Figure 15 Altered expression of the genes included in cluster III (1)

mRNA expression levels of genes included in cluster III under the indicated conditions were visualized using IGV.

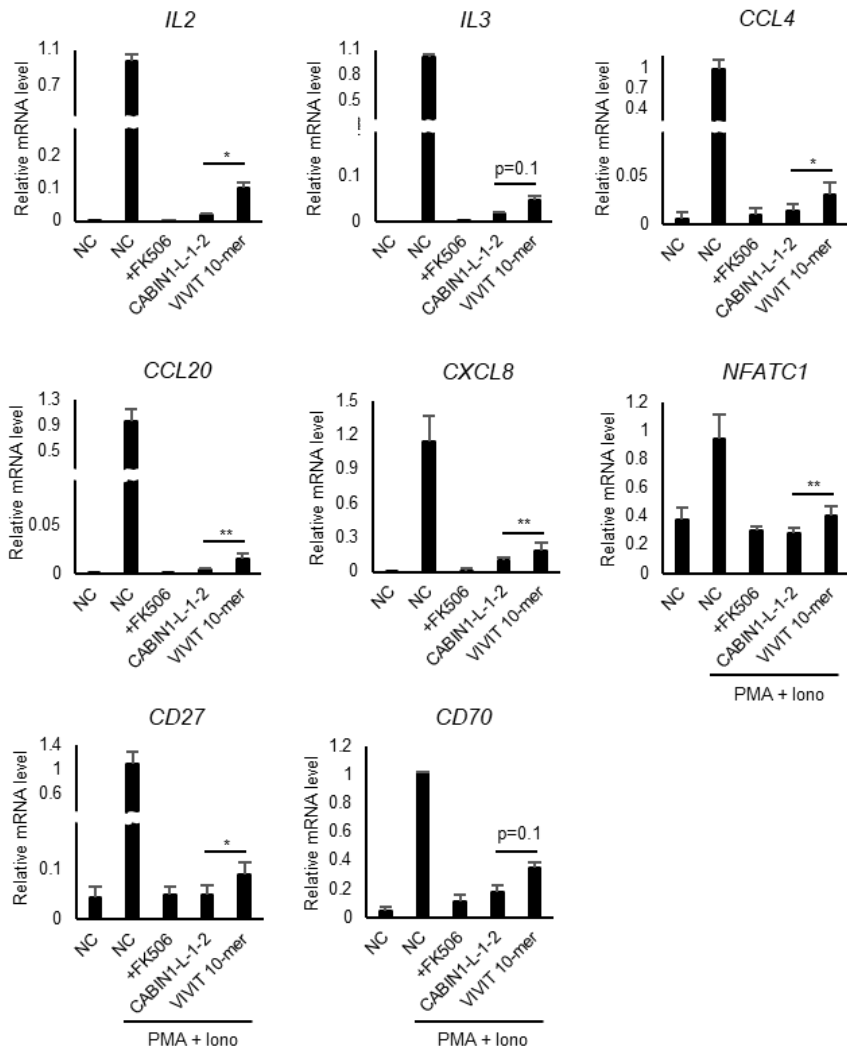


Figure 16 Altered expression of the genes included in cluster III (2)

The real-time quantitative PCR result of genes included in cluster III.

### **3–5. The CABIN1 peptide does not inhibit calcineurin phosphatase activity**

The VIVIT peptide binds to distinct regions of the CNA catalytic site and disrupts the CNA–NFAT interaction<sup>30</sup>. To confirm that the CABIN1 and VIVIT peptides have the same mechanism of action, we conducted a peptide competition assay. The CABIN1 peptide dose-dependently interfered with the interaction between the GST-tagged VIVIT peptide and His<sub>6</sub>-tagged CNA and vice versa (Figure 17). In contrast, neither CABIN1 nor VIVIT peptides diminished the binding affinity of NFATC2 or KSR2 fragments containing only the "LxVP" motif for CNA (Figure 18). These results suggest that the CABIN1 peptide only competes with the "PxIxIT" motif, like the VIVIT peptide.

Besides, ionomycin treatment did not affect the interaction between CNA and the CABIN1 or VIVIT peptide (Figure 19). This result suggests that the CABIN1 peptide, VIVIT peptide, and fused tag (GAL4 DBD) do not interfere with the active site of CNA. Next, we measured calcineurin phosphatase activity in Jurkat T cells expressing each peptide or treated with FK506 (Figure 20a). FK506, which interferes with the active site of CNA, decreased the phosphatase activity of CNA, but the CABIN1 and VIVIT peptides

did not. These peptides also did not reduce the phosphatase activity of CNA in vitro (Figure 20b).

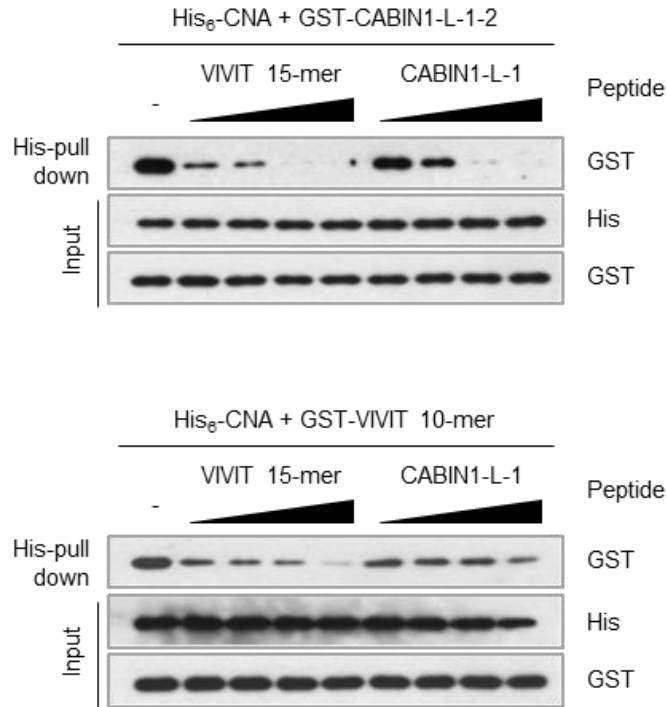


**Figure 17** The CABIN1 peptide binds to the same region of calcineurin as the VITIT peptide

In vitro peptide competition assay was conducted with VIVIT 15-mer and CABIN1-L-1 peptides in a dose-dependent manner. The molar ratios of the GST-tagged peptide to the competing peptide ranged from 1:50 to 1:400.

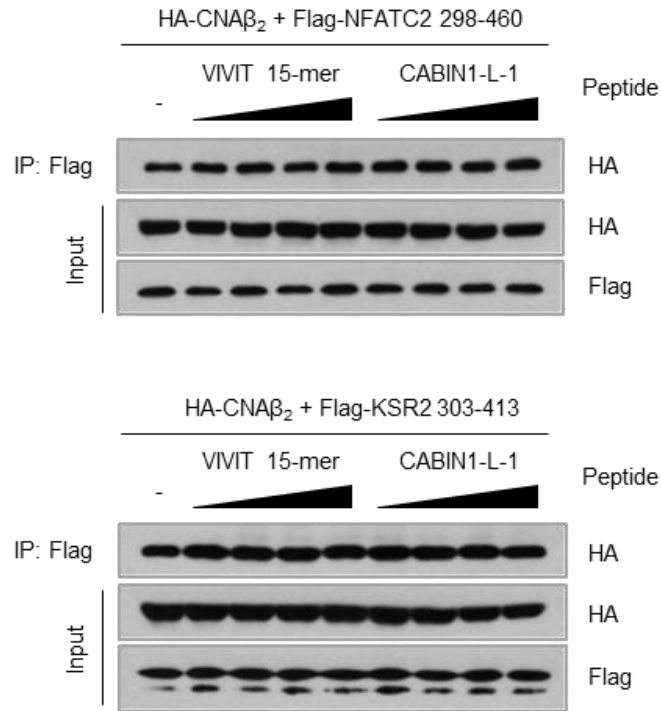


**Figure 18** The CABIN1 and VIVIT peptides do not affect the interaction between CNA and the “LxVP” motif

HEK293T cells were transfected with HA-CNA $\beta_2$  and Flag-NFATC2 or KSR2 fragment containing the “LxVP” motif. VIVIT 15-mer and CABIN1-L-1 peptides were added to the cell lysates in a dose-dependent manner (from 1  $\mu\text{M}$  to 64  $\mu\text{M}$ ) for competition. Immunoprecipitation was conducted with Flag antibody and co-precipitates was detected with HA antibody.

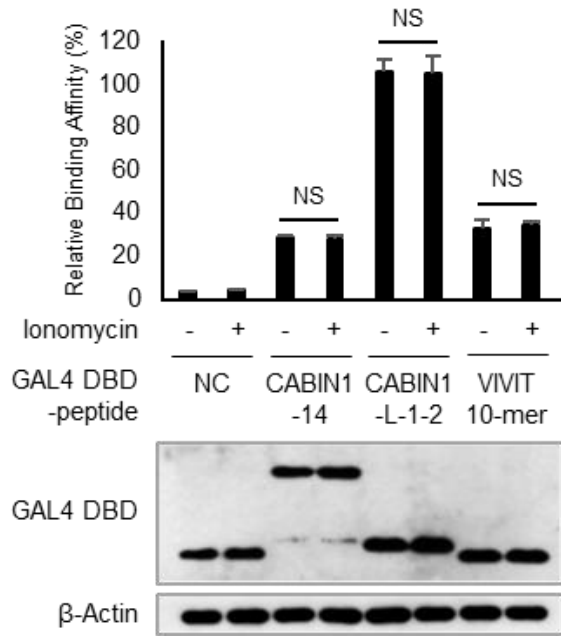


**Figure 19** The interaction between CNA and the CABIN1 fragment is not affected by ionomycin treatment

Mammalian two-hybrid assay was performed using VP16 AD-CNA $\beta_2$  and GAL4 DBD-peptides in HEK293T with or without 1  $\mu$ M ionomycin treatment. pM empty vector was used as a negative control. NS, non-significant, NC, negative control.

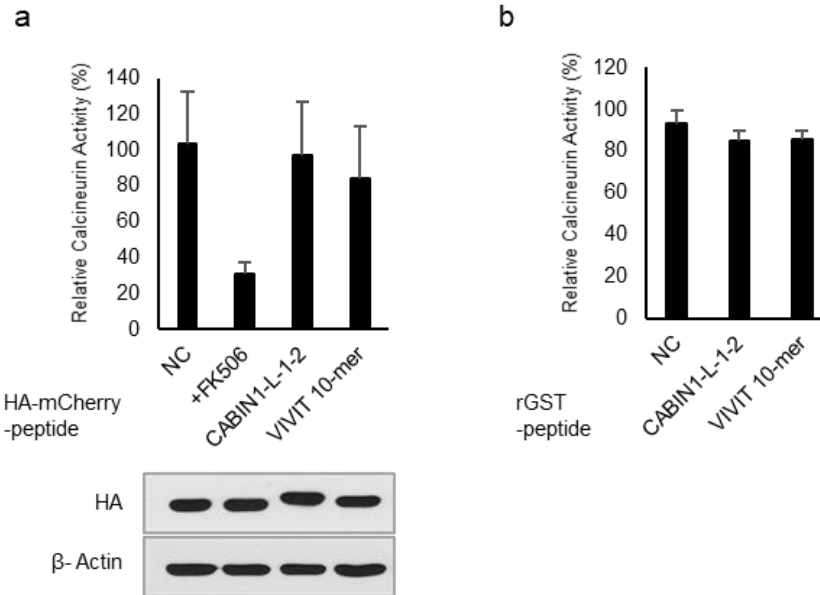


**Figure 20** The CABIN1 peptide does not inhibit calcineurin phosphatase activity

**a** Calcineurin cellular activity assay was performed using Jurkat T cells expressing HA-mCherry-peptides. Jurkat T cells expressing HA-mCherry were used as a negative control, and cells treated with FK506 used as a positive control. **b** In vitro calcineurin phosphatase activity assay using purified GST-peptides. Purified GST was used as a negative control. NS, non-significant, NC, negative control.

### **3-6. The C-terminal "PPTP" sequence is important for interaction with calcineurin**

To understand how the "PPTP" sequence contributes to the binding affinity to CNA, we compared the binding affinity of each GST-tagged peptide for CNA at the cellular level and in vitro (Figure 21). The "PPTP" sequence enhanced peptide's binding affinity to CNA only at the cellular level, not in vitro, suggesting that this was due to post-translational modifications (PTMs) on residues of "PPTP." Next, we substituted one or all of the "PPTP" residues with amino acids corresponding to each residue of the "GPHE" sequence of the VIVIT peptide. We conducted a mammalian two-hybrid assay using these constructs and CNA to determine which modification affected the affinity (Figure 22). As a result, all the substitutions dramatically disrupted the interaction with CNA, implying that every residue in the "PPTP" sequence is crucial for the interaction with CNA. This result suggests that the "PPTP" sequence could be a substrate motif of an upstream enzyme capable of modifying residues. Subsequent experiments using these substitutions revealed that threonine 9 and proline 10 of the CABIN1 peptide might be targets of PTM because, in vitro, peptides with substitutions at these residues exhibited binding affinities for CNA

comparable to that of wild-type CABIN1 peptide, while in cellular experiments, all the substitutions disrupted the interaction with calcineurin (Figure 23).

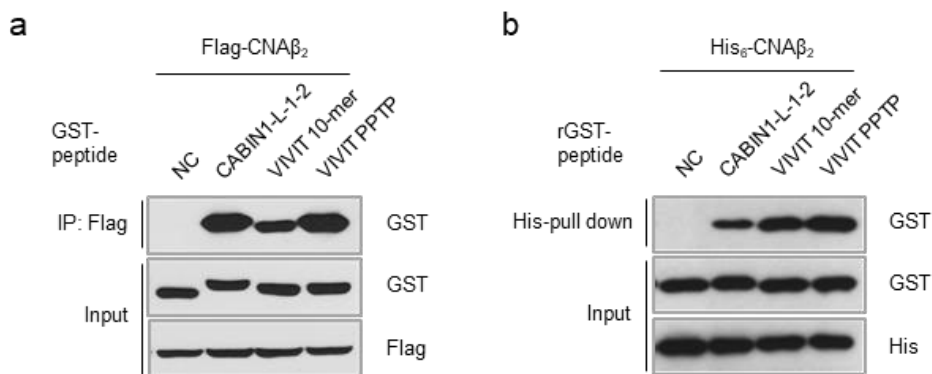


**Figure 21** The “PPTP” sequence is critical for the interaction with calcineurin in the cellular level

**a** HEK293T cells were transfected with Flag-CNA $\beta_2$  and GST-peptides. Immunoprecipitation assay was performed with Flag antibody and co-precipitates was detected with GST antibody. **b** In vitro His-pull down assay was performed using His $_6$ -CNA $\beta_2$  and GST-peptides. NC, negative control.

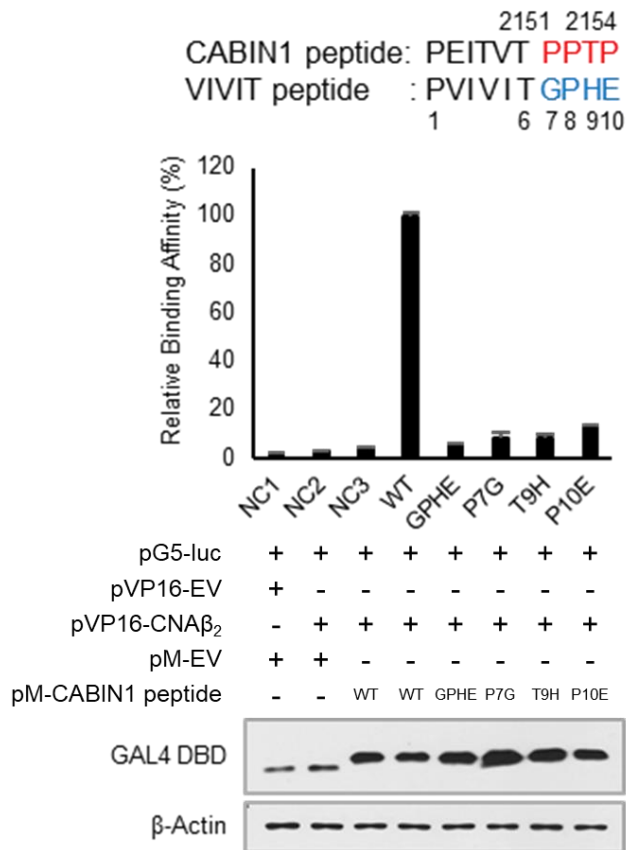
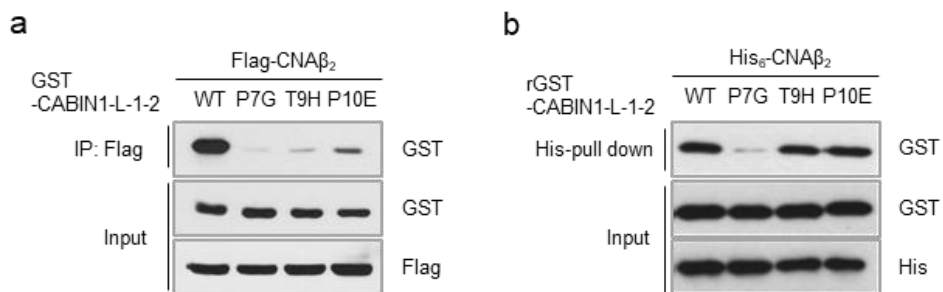


Figure 22 Binding affinity of the substituted CABIN1 peptides for calcineurin (1)

Mammalian two-hybrid assay was conducted using VP16 AD-CNA $\beta_2$  and GAL4 DBD-substituted CABIN1 peptides for verifying binding affinity in HEK293T cells. NC, negative control.



**Figure 23 Binding affinity of the substituted CABIN1 peptides for calcineurin (2)**

**a** HEK293T cells were transfected with Flag-CNA $\beta_2$  and GST-CABIN1 peptides. Immunoprecipitation assay was performed with Flag antibody and co-precipitates was detected with GST antibody. **b** In vitro His-pull down assay was performed using His<sub>6</sub>-CNA $\beta_2$  and GST-CABIN1 peptides.

### 3–7. Phosphorylation of CABIN1 T2154 is critical for the interaction with calcineurin

We investigated the phosphorylation and *O*-linked glycosylation of threonine residues and hydroxylation of proline residues of the peptides containing the “PPTP” sequence. First, we checked whether proline residues of the “PPTP” were hydroxylated. We treated Jurkat T cells expressing the mCherry-tagged CABIN1 peptide with dimethyloxalylglycine (DMOG), a prolyl hydroxylase inhibitor (Figure 24a, b). While DMOG stabilized hypoxia-inducible factor-1 alpha (HIF-1 $\alpha$ ), it did not affect the interaction between the CABIN1 peptides and CNA. Furthermore, we detected no hydroxyproline in the GST-tagged CABIN1 peptide or VIVIT peptide (Figure 24c). Next, we checked *O*-linked glycosylation at the threonine residue of the “PPTP” sequence. The *O*-linked glycosylation of the GST-tagged peptides containing the “PPTP” sequence (CABIN1-L-1-2 and VIVIT PPTP) was not higher than that of the negative control or VIVIT peptide, indicating that no *O*-linked glycosylation occurred in the “PPTP” sequence. (Figure 24c). Previous phosphoproteomics experiments reported the phosphorylation of threonine 2151 and threonine 2154 of the full-length CABIN1 during mitosis<sup>37</sup>. To identify the modified residue in

our model, we substituted each threonine with valine, which bears a methyl group instead of the hydroxyl group of threonine (Figure 25a). Substituting threonine 6 (threonine 2151 of the full-length CABIN1) with valine (T6V) abolished the interaction between the CABIN1 peptide and CNA in the cellular and in vitro experiments (Figure 25b). By contrast, substituting threonine 9 (threonine 2154 of the full-length CABIN1) with valine (T9V) abolished the interaction in the cellular experiment, not in vitro (Figure 25c). Moreover, the T9V substitution restored the CABIN1 peptide-suppressed transcriptional activity of NFAT more efficiently than the T6V substitution did (Figure 26). These results suggest that threonine 9 undergoes PTM, which increases the inhibitory effect on the calcineurin-NFAT pathway.

Indeed, we detected threonine 9 phosphorylation by western blot using an antibody against phospho-MAPK substrates (PXpTP) in Jurkat T cells expressing HA-mCherry-tagged peptides (Figure 27a). To directly identify the phosphorylated CABIN1 peptide in cells, we immunoprecipitated the HA-mCherry-tagged CABIN1 peptide with an anti-HA antibody from Jurkat T cells expressing the protein. We analyzed the purified protein with LC-MS/MS and observed threonine 9 phosphorylation (Figure 27b). Next, we synthesized a biotin-labeled VIVIT peptide, CABIN1 peptide, and

phosphorylated CABIN1 peptide. A biotin-pull down assay with these peptides showed that CABIN1 phosphorylation dramatically increased the affinity for CNA (Figure 28a). Finally, we quantitatively analyzed the binding affinity through surface plasma resonance (SPR). We observed that the phosphorylation of the 9th threonine of the CABIN1 peptide increased the binding affinity by about three-fold (Figure 28b). Collectively, these results demonstrate that the CABIN1 peptide is a more efficient *in vivo* inhibitor than the VIVIT peptide because the phosphorylation of the threonine in the “PPTP” sequence enhances the binding affinity for CNA.

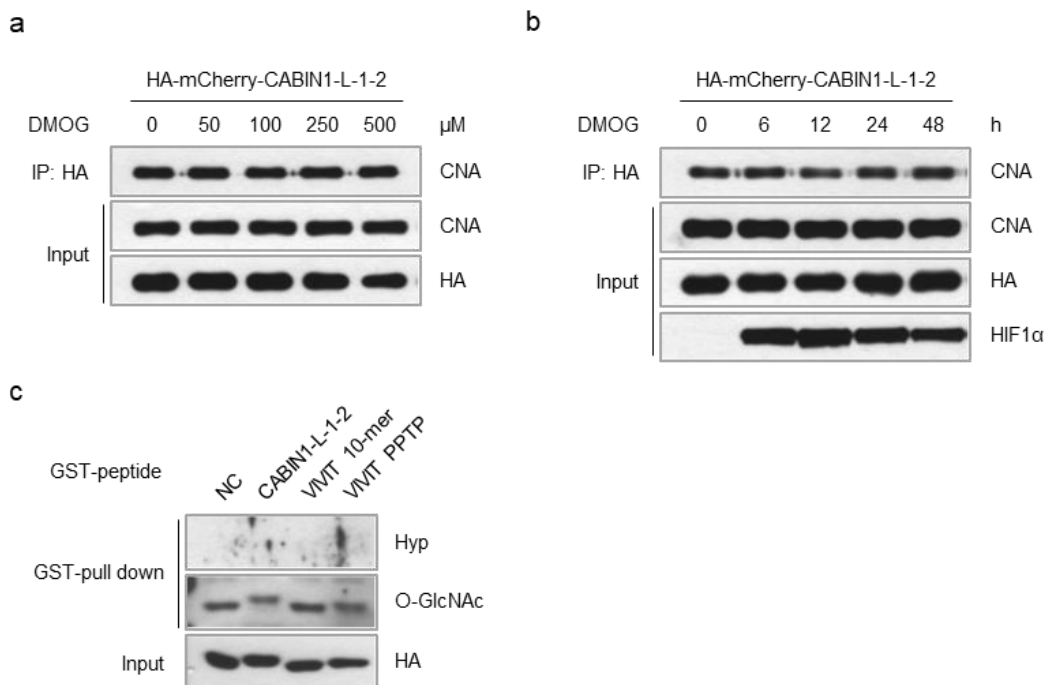


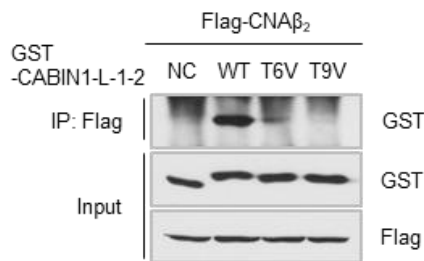
**Figure 24** No hydroxylation or O-GlcNAcylation occurred in the “PPTP” sequence

**a** Jurkat T cells expressing HA-mCherry-CABIN1 peptide were treated with DMOG in a dose-dependent manner for 12 h. **b** Jurkat T cells expressing HA-mCherry-CABIN1 peptide were treated with 500 μM DMOG in a time-dependent manner. Each cell lysate was immunoprecipitated with HA antibody and CABIN1 peptide-bound CNA was detected by western blotting. HIF-1α was detected as a positive control for DMOG treatment. **c** HEK293T cells were transfected with GST-peptides and GST-pull down assay was conducted. Hydroxyproline and O-linked glycosylation of the peptides were detected by western blotting. NC, negative control.

**a**

Label	Sequence
WT	PEITVTPPTP
T6V	PEITV <b>V</b> PPTP
T9V	PEITVTP <b>V</b> P

**b**



**c**

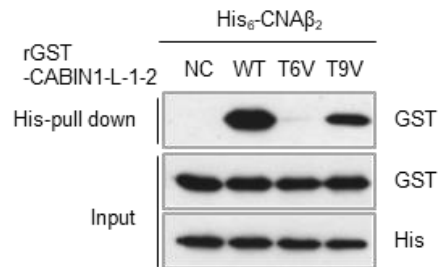


**Figure 25 Binding affinity of threonine to valine substitutions of the CABIN1 peptide for calcineurin**

**a** Amino acid sequence of threonine to valine substituted (TV) CABIN1 peptides. **b** HEK293T cells were transfected with Flag-CNA $\beta_2$  and GST-CABIN1 peptides. Immunoprecipitation assay was performed with Flag antibody and co-precipitates was detected with GST antibody. **c** In vitro His-pull down assay was performed using His<sub>6</sub>-CNA $\beta_2$  and GST-WT or TV CABIN1 peptides. NC, negative control, WT, wild-type.

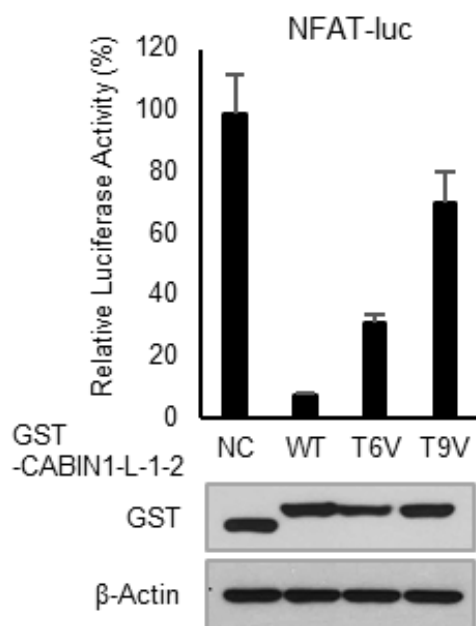


**Figure 26** TV substitution of the CABIN1 peptide restores the inhibitory effect on NFAT transcriptional activity

Luciferase reporter assay was performed to measure NFAT transcriptional activity in Jurkat T cells expressing GST–CABIN1 peptides under PMA and Ionomycin treatment. NC, negative control.

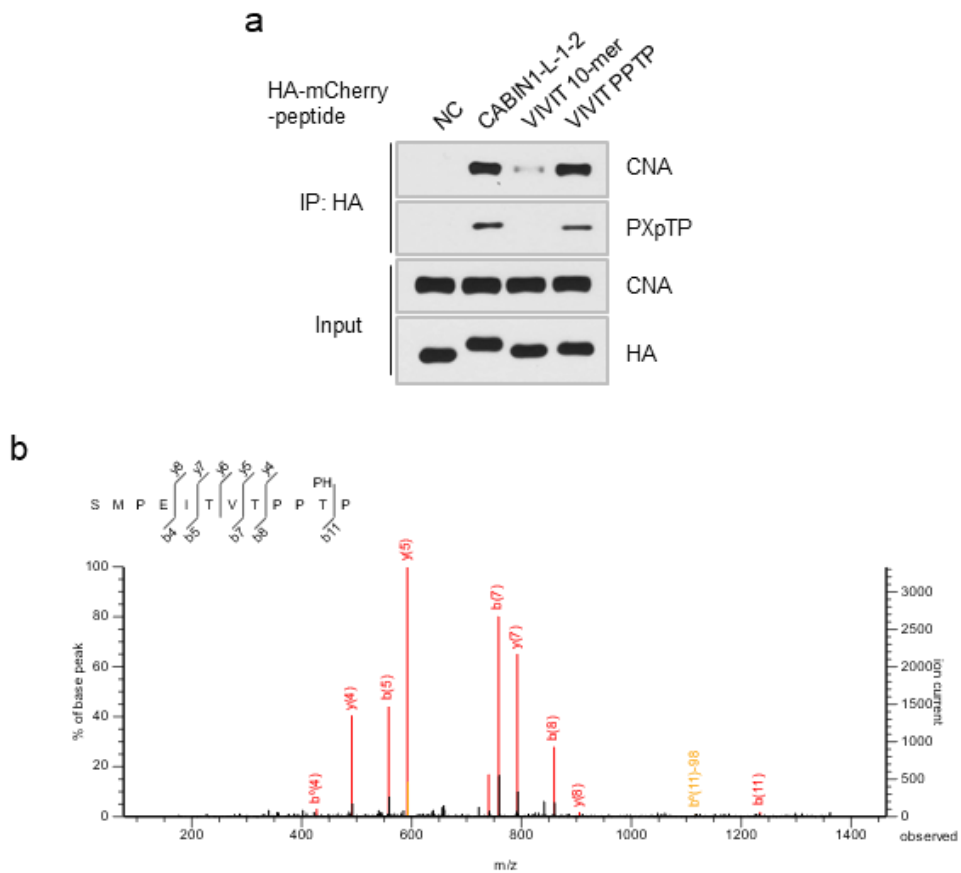


**Figure 27 Phosphorylation of the threonine in “PPTP” is detected at the cellular level**

**a** Immunoprecipitation assay in Jurkat T cells expressing HA–mCherry–peptides using HA antibody. Peptide–bound CNA and phosphorylated threonine were detected by western blotting. **b** Phosphorylation of the 9th threonine of the CABIN1 peptide (threonine 2154 of the full–length CABIN1) in Jurkat T cells was detected by LC–MS/MS.

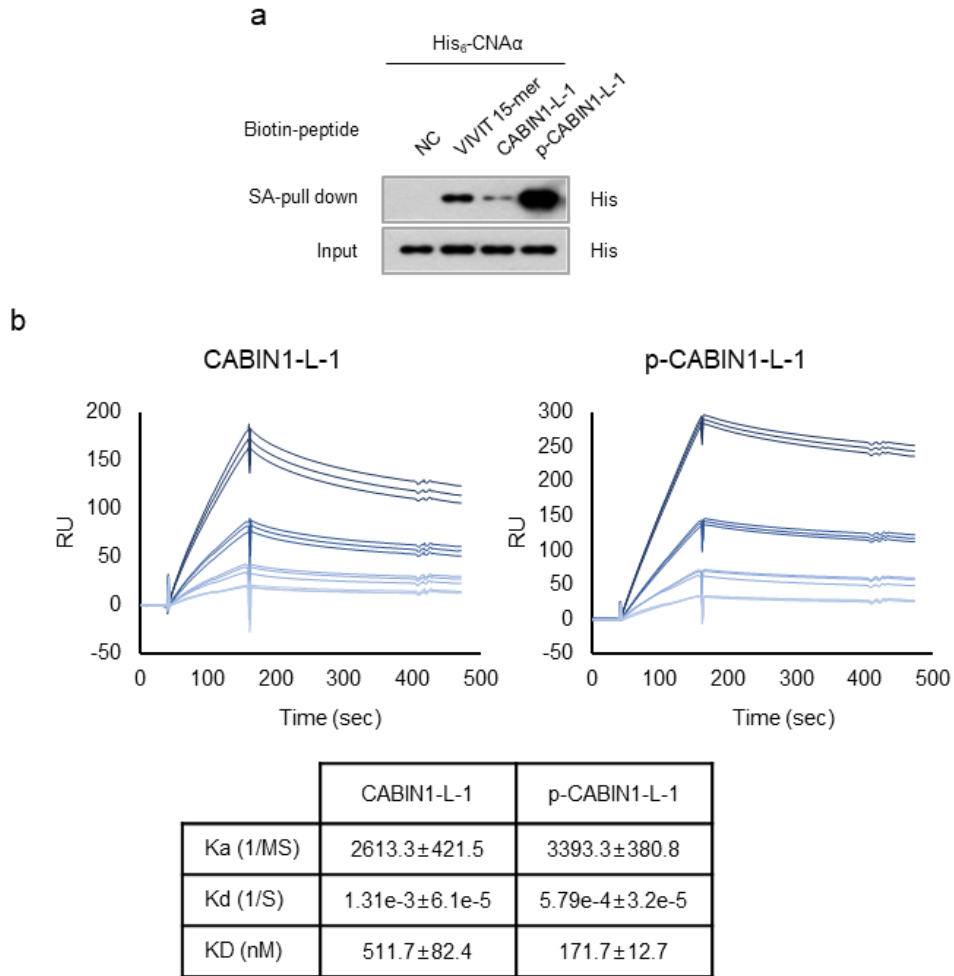


**Figure 28 Phosphorylation of CABIN1 T2154 enhances binding affinity for calcineurin**

**a** In vitro biotin-pull down assay was performed using streptavidin-conjugated agarose beads. Biotinylated peptide-bound CNA was detected with His antibody. VEET peptide was used as negative control. **b** CNA binding to biotinylated CABIN1 peptides with or without 9th threonine phosphorylation was measured by SPR. CNA concentrations ranged from 1.25, 2.5, 5, and 10 nM. Kinetics of interactions were calculated using the data of CABIN1 peptides captured cells minus negative control peptide captured cell. RU, response units, NC, negative control.

### 3–8. p38MAPK phosphorylates threonine 9 of the CABIN1 peptide

PMA, an activator of PKC, induces CABIN1 hyperphosphorylation, but PKC does not directly phosphorylate CABIN1<sup>29</sup>. Therefore, we investigated whether PMA causes the phosphorylation of the CABIN1 peptide (specifically the threonine of the “PPTP” sequence) and through which kinase. As a result of PMA treatment, CABIN1 peptide phosphorylation increased two hours after treatment (Figure 29a). To find kinases that can directly phosphorylate the CABIN1 peptide, we performed an in vitro phosphorylation assay with kinase candidates activated through PKC. We found that the MAPK family (ERK, JNK, and p38) and MKK4 directly phosphorylate the CABIN1 peptide (Figure 29b). We focused on the MAPKs, considering that the “PPTP” sequence is a perfectly suited substrate for this family. ERK2, JNK1, and p38  $\alpha$  phosphorylated the purified recombinant GST-tagged peptides containing the “PPTP” sequence (CABIN1-L-1-2 and VIVIT PPTP), but not the GST-tagged VIVIT peptide (Figure 29c). To investigate which kinase interacts with CABIN1 in nature, we conducted an immunoprecipitation assay. It revealed that only p38 $\alpha$  is bound to CABIN1 at the cellular level (Figure 30a). Besides, p38 $\alpha$

did not phosphorylate the substituted PPTP sequences in vitro (Figure 30b, c). We then confirmed that selective p38 inhibitors, such as EO 1428 or TAK 715, significantly reduced phosphorylation of the CABIN1 peptide, thereby decreasing its binding affinity for CNA (Figure 31a, b). These results suggest that p38 MAPK is an upstream kinase of the CABIN1 peptide in nature.

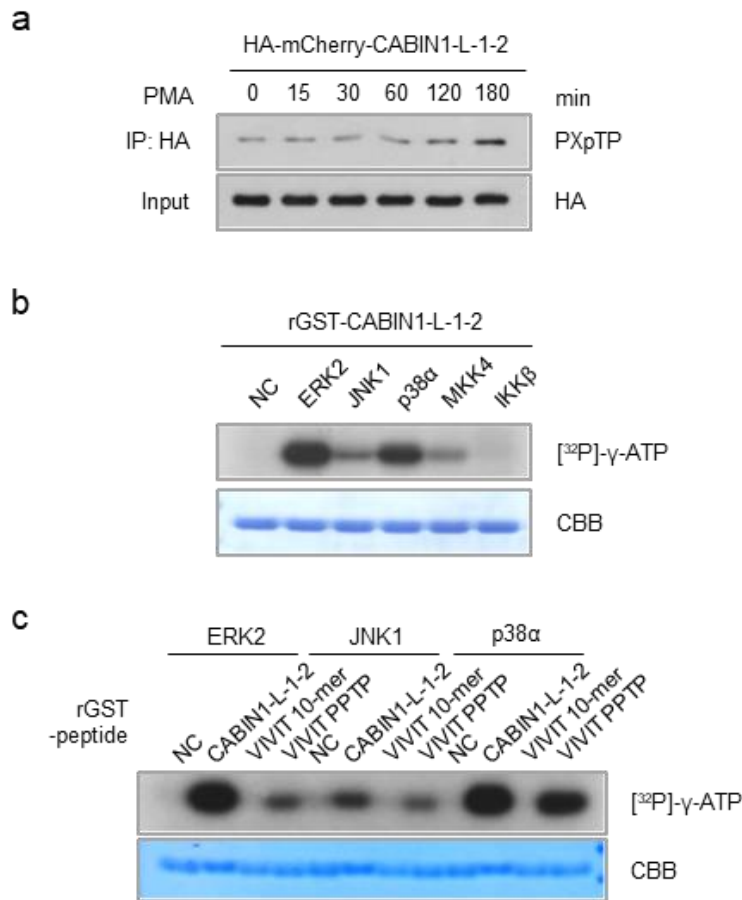


**Figure 29 Screening of putative upstream kinases of the CABIN1 peptide upon PMA treatment**

**a** Jurkat T cells expressing HA-mCherry-CABIN1 peptide were treated with 40 nM PMA in a time-dependent manner. Phosphorylated threonine of the immunoprecipitated peptide with HA antibody was detected with the [PXpTP] antibody. **b** In vitro kinase assay using purified GST-CABIN1 peptide and PKC downstream kinases. **c** In vitro kinase assay using purified GST-peptides and kinases included in the MAPK family. NC, negative control

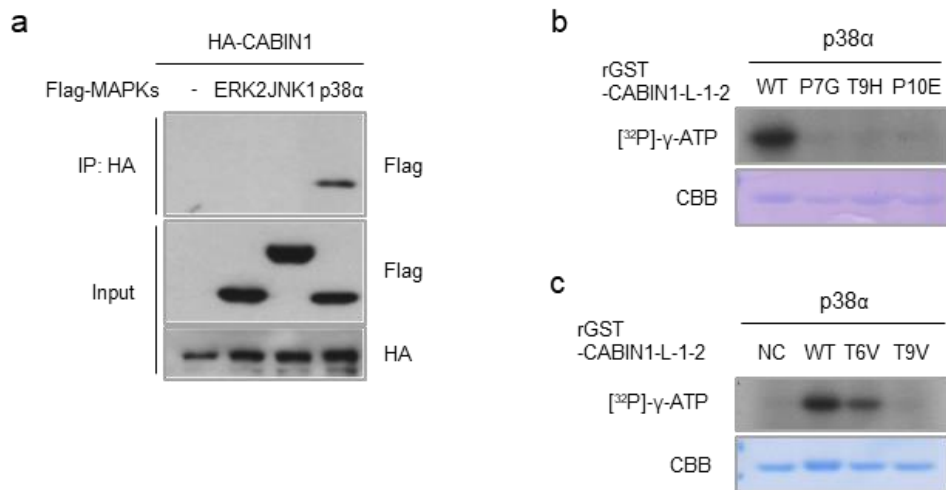


**Figure 30 p38 MAPK phosphorylates 9th threonine of the CABIN1 peptide**

**a** HEK293T cells were transfected with Flag-MAPKs and HA-CABIN1. Immunoprecipitation assay was performed with HA antibody and co-precipitates was detected with Flag antibody. **b, c** In vitro kinase assay using p38α and substituted CABIN1 peptides. WT, wild-type, NC, negative control.

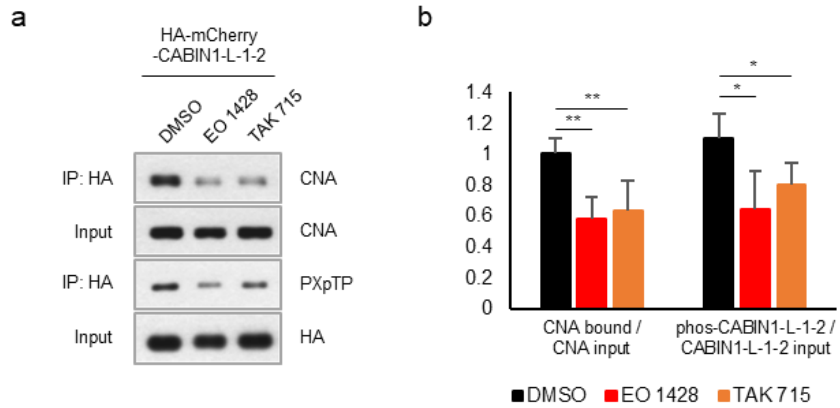


**Figure 31 p38 MAPK inhibitors reduce phosphorylation of the CABIN1 peptide and interaction with CNA**

**a** Jurkat T cells expressing HA-mCherry-CABIN1 peptide were treated with 10  $\mu$ M p38 $\alpha$  inhibitors for 16 h. Immunoprecipitation was performed with HA antibody and detected by western blotting. **b** Phosphorylated threonine and peptide-bound CNA of **a** were measured using imageJ, and the ratio of phosphorylation and calcineurin binding to CABIN1 peptide were calculated.

## VI. DISCUSSION

Long-term treatment with FK506 or cyclosporin A increases the expression of TGF- $\beta$  and pro-fibrogenic genes such as collagen, fibronectin, and metalloproteinases<sup>38</sup>. Consequently, these drugs cause severe side effects, such as nephrotoxicity, fibrogenesis, neurotoxicity, and diabetes<sup>27</sup>. To overcome these side effects, alternative inhibitors that specifically perturb the calcineurin-NFAT pathway have been developed. Among them, the VIVIT peptide showed better results than FK506 in mouse transplantation model and various disease models regulated by the calcineurin-NFAT pathway<sup>39-41</sup>.

However, some characteristics of the VIVIT peptide (such as its stability, and affinity) and peptide drug delivery systems require improvement before they reach clinical use<sup>19</sup>. At present, a few studies reported attempts at improving the VIVIT peptide. Most of them related to delivery systems, such as conjugation with various cell-penetrating peptides or using viral delivery systems<sup>39,42-44</sup>. On the other hand, reports on VIVIT peptide binding affinity improvement are rare. In 2014, Qian, Dougherty et al. reported that the artificial peptidyl inhibitor ZIZIT-cisPro had a better binding affinity than the VIVIT peptide<sup>31</sup>. However, since the ZIZIT-cisPro does not exist in nature, it could trigger an immune response.

This study identified a key peptide sequence in the C-terminal fragment of CABIN1 that inhibited the calcineurin–NFAT pathway and clarified its mechanism. Based on this study, the CABIN1 peptide has two advantages over the VIVIT peptide. First, the CABIN1 peptide has a higher binding affinity for calcineurin than the VIVIT peptide. The CABIN1 peptide contains an N-terminal “PxIxIT” motif and a “PPTP” sequence, which is different from the C-terminal “GPHEE” sequence of the VIVIT peptide. The C-terminal “PPTP” sequence endows this peptide with a higher affinity for CNA than the VIVIT peptide (Figure 8b). This higher affinity for calcineurin allows the CABIN1 peptide to better disrupt the interaction between calcineurin and NFAT, ultimately blocking NFAT dephosphorylation and nuclear translocation more efficiently than the VIVIT peptide (Figure 12b, 13b). Thus, the CABIN1 peptide successfully suppresses the expression of NFAT target genes upon T cell activation much more efficiently than the VIVIT peptide does (Figure 16). These results suggest that the CABIN1 peptide is a more efficient calcineurin inhibitor than the VIVIT peptide. However, the CABIN1 peptide only had a higher affinity at the cellular level, not in vitro (Figure 21a, b) meaning that the CABIN1 peptide undergoes PTM that affects its binding affinity. Recent studies suggested the importance of a phosphorylated serine

or threonine in calcineurin inhibitory peptides<sup>20,45</sup>. However, no one has directly demonstrated their existence or role in nature. Here, we directly revealed the phosphorylation of the threonine of the “PPTP” sequence (T9) via LC-MS/MS (Figure 27b) and quantitatively demonstrated that it increases the binding affinity to calcineurin (Figure 28b). During Jurkat T cell activation, the phosphorylation of nuclear NFAT and CABIN1 peptides by p38 MAPK may cooperatively attenuate the immune response by inhibiting the re-importation of phosphorylated NFAT into the nucleus.

Second, the CABIN1 peptide is more stable than the full-length VIVIT peptide (15-mer) under physiological conditions. While comparing the VIVIT 15-mer with the VIVIT decamer, we found an interesting feature of the VIVIT peptide. The mCherry-tagged VIVIT peptide was dramatically less stable when repeated C-terminal glutamate (Figure 10b, c). The C-terminal glutamine repeat is the C-terminal degron targeted by the CUL4/DCAF12 ubiquitin ligase complex<sup>46</sup>. Accordingly, when using the full-length VIVIT peptide, the tag type or location should be considered.

As an alternative calcineurin inhibitor, the CABIN1 peptide may exhibit advantages similar to the VIVIT peptide. These peptides compete to interact with the CNA, implying that they bind to the

same region and have the same mode of action (Figure 17). Since the CABIN1 peptide does not affect calcineurin's phosphatase activity (Figure 20a, b), it probably does not perturb the dephosphorylation of other calcineurin substrates except NFAT. For instance, KSR2, another calcineurin substrate that interacts with calcineurin via the "LxVP" motif, is dephosphorylated by calcineurin in response to glucose stimulation. Dephosphorylated KSR2 induces ERK activation and insulin secretion<sup>9</sup>. Because the CABIN1 and VIVIT peptides only carry the "PxIxIT" motif and not the "LxVP" motif, they do not interfere with the interaction between KSR2 and calcineurin (Figure 18, bottom). A previous report showed that the VIVIT peptide did not decrease insulin secretion in allogeneic islet transplantation in mice<sup>39</sup>, supporting this assumption. Collectively, the CABIN1 peptide is expected to be less toxic calcineurin inhibitor that does not inhibit insulin secretion and does not induce diabetes like VIVIT peptide.

In addition, VIVIT peptide showed a better performance to prevent restenosis and cardiac hypertrophy than conventional inhibitors. Unlike CsA or FK506, the VIVIT peptide doesn't affect the transcriptional activity of NF $\kappa$ B in RAW 264.7 macrophages, and barely affect endothelial wound healing and TGF- $\beta$  expression<sup>47</sup>. The VIVIT peptide induce cardiac myocyte apoptosis, which is

expected to help fight cardiac hypertrophy<sup>48</sup>. Furthermore, VIVIT peptide combined with dNP2, a blood–brain barrier–penetrating peptide, selectively inhibited Th1 and Th17 cells, but not regulatory T cells, whereas CsA inhibited all subsets of T cell<sup>44</sup>. Because the CABIN1 peptide has the same mode of action as the VIVIT peptide, the CABIN1 peptide is expected to show similar results to the VIVIT peptide.

The present study found putative calcineurin target genes, such as *NINJI* and *ZP4*, that are not regulated via the calcineurin–NFAT pathway. Upon T cell activation, these genes were repressed by FK506 but unaffected by the CABIN1 and VIVIT peptides (Figure 32a, b). *NINJI* encodes Ninjurin–1, a transmembrane adhesion molecule involved in axonal growth, inflammation, and cell death<sup>49,50</sup>. Ninjurin–1 regulates inflammatory activation by modulating Toll–like receptor 4 signaling through direct binding to lipopolysaccharides in macrophages<sup>51</sup>. *ZP4*, a component of the zona pellucida glycoproteins, promotes T cell proliferation<sup>52</sup>. Further studies should confirm whether these genes are associated with the side effects of FK506.

The interactive mechanism between calcineurin and its binding partners has not been fully elucidated. Besides CABIN1, other calcineurin binding partners, such as AKAP79, RCAN1, and TRESK,

carry a “PxIxIT” motif<sup>1</sup> (Figure 3a). However, we found no reports investigating potential PTMs for their calcineurin binding regions. Our previous study showed that an internal fragment of CABIN1 that does not contain the “PxIxIT” and “LxVP” motif also inhibits calcineurin<sup>53</sup>. Here, we revealed the detailed mechanism of CABIN1 as a calcineurin inhibitor and proved the superiority of the CABIN1 peptide over the VIVIT peptide for the first time. Modulation of the inhibitory effect through phosphorylation can be an advantage. Phosphorylation acts as a switch for the CABIN1 peptide, allowing it to target cells or tissues where p38 MAPK is highly activated. Given that the NFAT family contributes to the progression and metastasis of many cancers<sup>54</sup>, the CABIN1 peptide could be used as an anticancer agent. Finally, our findings provide an alternative therapeutic strategy against the various diseases related to the calcineurin–NFAT pathway.

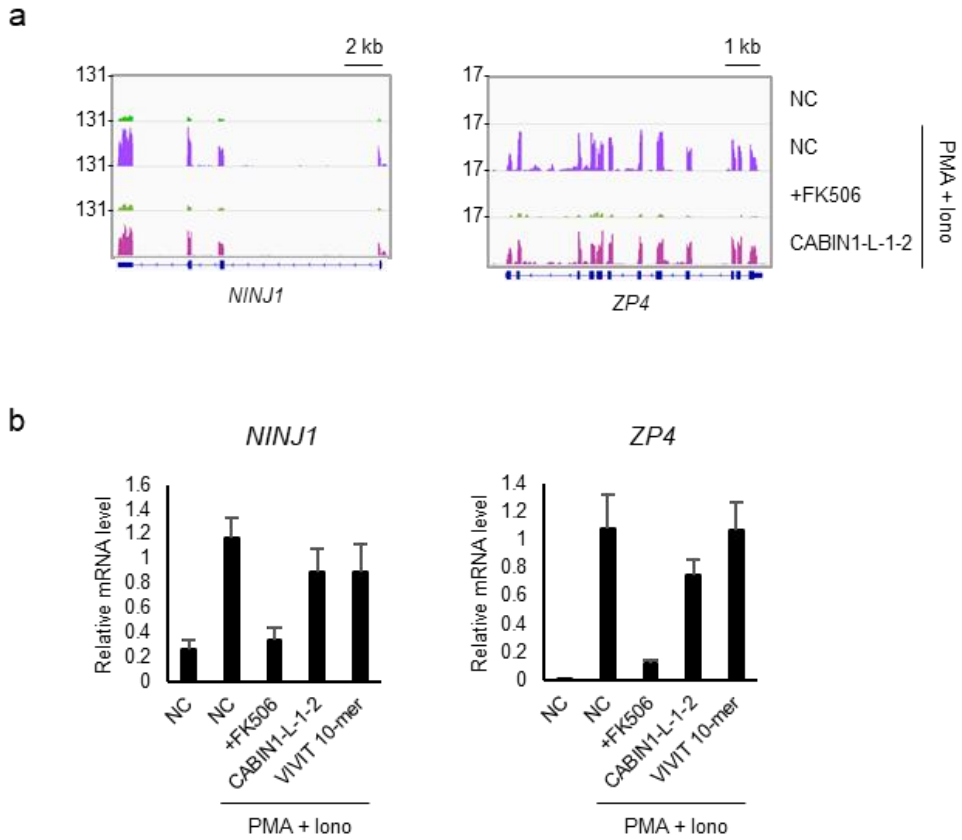


**Figure 32 Putative calcineurin target genes that are not regulated via the calcineurin–NFAT pathway**

**a** mRNA expression levels of genes repressed by FK506 but unaffected by the CABIN1 peptide. **b** The real–time quantitative PCR result of genes of **a**. NC, negative control.

## VI. REFERENCES

- 1 Li, H., Rao, A. & Hogan, P. G. Interaction of calcineurin with substrates and targeting proteins. *Trends Cell Biol* **21**, 91–103, doi:10.1016/j.tcb.2010.09.011 (2011).
- 2 Li, S. J. *et al.* Cooperative autoinhibition and multi-level activation mechanisms of calcineurin. *Cell Res* **26**, 336–349, doi:10.1038/cr.2016.14 (2016).
- 3 Rusnak, F. & Mertz, P. Calcineurin: form and function. *Physiol Rev* **80**, 1483–1521, doi:10.1152/physrev.2000.80.4.1483 (2000).
- 4 Gallagher, S. C. *et al.* There is communication between all four Ca(2+)–bindings sites of calcineurin B. *Biochemistry* **40**, 12094–12102, doi:10.1021/bi0025060 (2001).
- 5 Stemmer, P. M. & Klee, C. B. Dual calcium ion regulation of calcineurin by calmodulin and calcineurin B. *Biochemistry* **33**, 6859–6866, doi:10.1021/bi00188a015 (1994).
- 6 Yang, S. A. & Klee, C. B. Low affinity Ca<sup>2+</sup>–binding sites of calcineurin B mediate conformational changes in calcineurin A. *Biochemistry* **39**, 16147–16154, doi:10.1021/bi001321q (2000).
- 7 Crabtree, G. R. & Clipstone, N. A. Signal transmission between the plasma membrane and nucleus of T lymphocytes.

- Annu Rev Biochem* **63**, 1045–1083,  
doi:10.1146/annurev.bi.63.070194.005145 (1994).
- 8 Schulz, R. A. & Yutzey, K. E. Calcineurin signaling and NFAT activation in cardiovascular and skeletal muscle development. *Dev Biol* **266**, 1–16, doi:10.1016/j.ydbio.2003.10.008 (2004).
- 9 Dougherty, M. K. *et al.* KSR2 is a calcineurin substrate that promotes ERK cascade activation in response to calcium signals. *Mol Cell* **34**, 652–662,  
doi:10.1016/j.molcel.2009.06.001 (2009).
- 10 Baumgartel, K. & Mansuy, I. M. Neural functions of calcineurin in synaptic plasticity and memory. *Learn Mem* **19**, 375–384, doi:10.1101/lm.027201.112 (2012).
- 11 Schwartz, R. H. Models of T cell anergy: is there a common molecular mechanism? *J Exp Med* **184**, 1–8,  
doi:10.1084/jem.184.1.1 (1996).
- 12 Macian, F. *et al.* Transcriptional mechanisms underlying lymphocyte tolerance. *Cell* **109**, 719–731,  
doi:10.1016/s0092-8674(02)00767-5 (2002).
- 13 Loh, C., Carew, J. A., Kim, J., Hogan, P. G. & Rao, A. T-cell receptor stimulation elicits an early phase of activation and a later phase of deactivation of the transcription factor NFAT1.

- Mol Cell Biol* **16**, 3945–3954, doi:10.1128/MCB.16.7.3945 (1996).
- 14 Su, B. *et al.* JNK is involved in signal integration during costimulation of T lymphocytes. *Cell* **77**, 727–736, doi:10.1016/0092–8674(94)90056–6 (1994).
- 15 Harhaj, E. W. & Sun, S. C. IkappaB kinases serve as a target of CD28 signaling. *J Biol Chem* **273**, 25185–25190, doi:10.1074/jbc.273.39.25185 (1998).
- 16 Rao, A., Luo, C. & Hogan, P. G. Transcription factors of the NFAT family: regulation and function. *Annu Rev Immunol* **15**, 707–747, doi:10.1146/annurev.immunol.15.1.707 (1997).
- 17 Tordai, A., Sarkadi, B., Gorog, G. & Gardos, G. Inhibition of the CD3–mediated calcium signal by protein kinase C activators in human T (Jurkat) lymphoblastoid cells. *Immunol Lett* **20**, 47–52, doi:10.1016/0165–2478(89)90067–9 (1989).
- 18 Gomez del Arco, P., Martinez–Martinez, S., Maldonado, J. L., Ortega–Perez, I. & Redondo, J. M. A role for the p38 MAP kinase pathway in the nuclear shuttling of NFATp. *J Biol Chem* **275**, 13872–13878, doi:10.1074/jbc.275.18.13872 (2000).

- 19 Yu, H., van Berkel, T. J. & Biessen, E. A. Therapeutic potential of VIVIT, a selective peptide inhibitor of nuclear factor of activated T cells, in cardiovascular disorders. *Cardiovasc Drug Rev* **25**, 175–187, doi:10.1111/j.1527–3466.2007.00011.x (2007).
- 20 Nakamura, T. *et al.* Overexpression of C16orf74 is involved in aggressive pancreatic cancers. *Oncotarget* **8**, 50460–50475, doi:10.18632/oncotarget.10912 (2017).
- 21 Okamura, H. *et al.* Concerted dephosphorylation of the transcription factor NFAT1 induces a conformational switch that regulates transcriptional activity. *Mol Cell* **6**, 539–550, doi:10.1016/s1097–2765(00)00053–8 (2000).
- 22 Liu, J. O., Nacev, B. A., Xu, J. & Bhat, S. It takes two binding sites for calcineurin and NFAT to tango. *Mol Cell* **33**, 676–678, doi:10.1016/j.molcel.2009.03.005 (2009).
- 23 Macian, F. NFAT proteins: key regulators of T–cell development and function. *Nat Rev Immunol* **5**, 472–484, doi:10.1038/nri1632 (2005).
- 24 Rodriguez, A. *et al.* A conserved docking surface on calcineurin mediates interaction with substrates and immunosuppressants. *Mol Cell* **33**, 616–626, doi:10.1016/j.molcel.2009.01.030 (2009).

- 25 Griffith, J. P. *et al.* X-ray structure of calcineurin inhibited by the immunophilin-immunosuppressant FKBP12-FK506 complex. *Cell* **82**, 507–522, doi:10.1016/0092-8674(95)90439-5 (1995).
- 26 Jin, L. & Harrison, S. C. Crystal structure of human calcineurin complexed with cyclosporin A and human cyclophilin. *Proc Natl Acad Sci U S A* **99**, 13522–13526, doi:10.1073/pnas.212504399 (2002).
- 27 Azzi, J. R., Sayegh, M. H. & Mallat, S. G. Calcineurin inhibitors: 40 years later, can't live without. *J Immunol* **191**, 5785–5791, doi:10.4049/jimmunol.1390055 (2013).
- 28 Aramburu, J. *et al.* Affinity-driven peptide selection of an NFAT inhibitor more selective than cyclosporin A. *Science* **285**, 2129–2133, doi:10.1126/science.285.5436.2129 (1999).
- 29 Sun, L. *et al.* Cabin 1, a negative regulator for calcineurin signaling in T lymphocytes. *Immunity* **8**, 703–711, doi:10.1016/s1074-7613(00)80575-0 (1998).
- 30 Takeuchi, K., Roehrl, M. H., Sun, Z. Y. & Wagner, G. Structure of the calcineurin-NFAT complex: defining a T cell activation switch using solution NMR and crystal

- coordinates. *Structure* **15**, 587–597,  
doi:10.1016/j.str.2007.03.015 (2007).
- 31 Qian, Z. *et al.* Structure–based optimization of a peptidyl inhibitor against calcineurin–nuclear factor of activated T cell (NFAT) interaction. *J Med Chem* **57**, 7792–7797,  
doi:10.1021/jm500743t (2014).
- 32 Manders, E. M., Stap, J., Brakenhoff, G. J., van Driel, R. & Aten, J. A. Dynamics of three–dimensional replication patterns during the S–phase, analysed by double labelling of DNA and confocal microscopy. *J Cell Sci* **103 ( Pt 3)**, 857–862, doi:10.1242/jcs.103.3.857 (1992).
- 33 Bolte, S. & Cordelieres, F. P. A guided tour into subcellular colocalization analysis in light microscopy. *J Microsc* **224**, 213–232, doi:10.1111/j.1365–2818.2006.01706.x (2006).
- 34 Dobin, A. *et al.* STAR: ultrafast universal RNA–seq aligner. *Bioinformatics* **29**, 15–21, doi:10.1093/bioinformatics/bts635 (2013).
- 35 de Hoon, M. J., Imoto, S., Nolan, J. & Miyano, S. Open source clustering software. *Bioinformatics* **20**, 1453–1454,  
doi:10.1093/bioinformatics/bth078 (2004).
- 36 Aramburu, J., Azzoni, L., Rao, A. & Perussia, B. Activation and expression of the nuclear factors of activated T cells,

- NFATp and NFATc, in human natural killer cells: regulation upon CD16 ligand binding. *J Exp Med* **182**, 801–810, doi:10.1084/jem.182.3.801 (1995).
- 37 Olsen, J. V. *et al.* Quantitative phosphoproteomics reveals widespread full phosphorylation site occupancy during mitosis. *Sci Signal* **3**, ra3, doi:10.1126/scisignal.2000475 (2010).
- 38 Khanna, A., Plummer, M., Bromberek, C., Bresnahan, B. & Hariharan, S. Expression of TGF- $\beta$  and fibrogenic genes in transplant recipients with tacrolimus and cyclosporine nephrotoxicity. *Kidney Int* **62**, 2257–2263, doi:10.1046/j.1523-1755.2002.00668.x (2002).
- 39 Noguchi, H. *et al.* A new cell-permeable peptide allows successful allogeneic islet transplantation in mice. *Nat Med* **10**, 305–309, doi:10.1038/nm994 (2004).
- 40 Liu, Z., Zhang, C., Dronadula, N., Li, Q. & Rao, G. N. Blockade of nuclear factor of activated T cells activation signaling suppresses balloon injury-induced neointima formation in a rat carotid artery model. *J Biol Chem* **280**, 14700–14708, doi:10.1074/jbc.M500322200 (2005).
- 41 Kuriyama, M. *et al.* A cell-permeable NFAT inhibitor peptide prevents pressure-overload cardiac hypertrophy. *Chem Biol*

- Drug Des* **67**, 238–243, doi:10.1111/j.1747–0285.2006.00360.x (2006).
- 42 Peuker, K. *et al.* Epithelial calcineurin controls microbiota–dependent intestinal tumor development. *Nat Med* **22**, 506–515, doi:10.1038/nm.4072 (2016).
- 43 Choi, J. M., Sohn, J. H., Park, T. Y., Park, J. W. & Lee, S. K. Cell permeable NFAT inhibitory peptide Sim–2–VIVIT inhibits T–cell activation and alleviates allergic airway inflammation and hyper–responsiveness. *Immunol Lett* **143**, 170–176, doi:10.1016/j.imlet.2012.01.016 (2012).
- 44 Lee, H. G., Kim, L. K. & Choi, J. M. NFAT–Specific Inhibition by dNP2–VIVITAmeliorates Autoimmune Encephalomyelitisby Regulation of Th1 and Th17. *Mol Ther Methods Clin Dev* **16**, 32–41, doi:10.1016/j.omtm.2019.10.006 (2020).
- 45 Nguyen, H. Q. *et al.* Quantitative mapping of protein–peptide affinity landscapes using spectrally encoded beads. *Elife* **8**, doi:10.7554/eLife.40499 (2019).
- 46 Koren, I. *et al.* The Eukaryotic Proteome Is Shaped by E3 Ubiquitin Ligases Targeting C–Terminal Degrons. *Cell* **173**, 1622–1635 e1614, doi:10.1016/j.cell.2018.04.028 (2018).

- 47 Yu, H. *et al.* Therapeutic potential of a synthetic peptide inhibitor of nuclear factor of activated T cells as antirestenotic agent. *Arterioscler Thromb Vasc Biol* **26**, 1531–1537, doi:10.1161/01.ATV.0000225286.30710.af (2006).
- 48 Pu, W. T., Ma, Q. & Izumo, S. NFAT transcription factors are critical survival factors that inhibit cardiomyocyte apoptosis during phenylephrine stimulation in vitro. *Circ Res* **92**, 725–731, doi:10.1161/01.RES.0000069211.82346.46 (2003).
- 49 Araki, T. & Milbrandt, J. Ninjurin, a novel adhesion molecule, is induced by nerve injury and promotes axonal growth. *Neuron* **17**, 353–361, doi:10.1016/s0896–6273(00)80166–x (1996).
- 50 Kayagaki, N. *et al.* NINJ1 mediates plasma membrane rupture during lytic cell death. *Nature* **591**, 131–136, doi:10.1038/s41586–021–03218–7 (2021).
- 51 Shin, M. W. *et al.* Ninjurin1 regulates lipopolysaccharide–induced inflammation through direct binding. *Int J Oncol* **48**, 821–828, doi:10.3892/ijo.2015.3296 (2016).
- 52 Choudhury, S., Ganguly, A., Chakrabarti, K., Sharma, R. K. & Gupta, S. K. DNA vaccine encoding chimeric protein encompassing epitopes of human ZP3 and ZP4:

- immunogenicity and characterization of antibodies. *J Reprod Immunol* **79**, 137–147, doi:10.1016/j.jri.2008.09.002 (2009).
- 53 Jang, H., Cho, E. J. & Youn, H. D. A new calcineurin inhibition domain in Cabin1. *Biochem Biophys Res Commun* **359**, 129–135, doi:10.1016/j.bbrc.2007.05.066 (2007).
- 54 Mancini, M. & Toker, A. NFAT proteins: emerging roles in cancer progression. *Nat Rev Cancer* **9**, 810–820, doi:10.1038/nrc2735 (2009).

## VII. ABSTRACT IN KOREAN

## 국문초록

# CABIN1 펩타이드를 이용한 대체 calcineurin 억제제 개발

이상호

분자의학 및 바이오제약학과

CABIN1 단백질의 카르복실 말단 조각은 calcineurin 과 상호작용하여 T 세포 활성화에 필수적인 NFAT 의 전사활성을 억제한다. 하지만 calcineurin 과 결합하는 정확한 아미노산 서열과 그 기전에 대해서는 아직 밝혀지지 않았다. 본 연구는 CABIN1 의 카르복실 말단 조각과 calcineurin 의 결합에 있어 최소한 CABIN1 의 2146 번부터 2155 번까지 10 개 아미노산이 필요하다는 것을 입증하였다. 이 펩타이드는 아미노 말단에 “PxIxIT” 모티프를 가지고, 카르복실 말단에 고유한 “PPTP” 서열을 갖는다. 생리적인 환경에서 p38 MAPK 는 “PPTP”서열의 트레오닌 잔기를 인산화 시키고, 이는 CABIN1 펩타이드의 calcineurin 에 대한 결합력을 상당히 향상시킨다. 그로 인해 CABIN1 펩타이드는 calcineurin 의 탈인산화 효소활성에 영향을 주지 않으면서 VIVIT 펩타이드보다 더 효과적으로 calcineurin-NFAT 경로와 T 세포의 활성을 억제한다. 결과적으로, CABIN1 펩타이드는 대체 calcineurin

억제제로서 큰 잠재력을 가지고 있고, calcineurin-NFAT 경로에 의해 유발되는 다양한 질병에 대한 새로운 치료기회를 제공할 수 있을 것이다.

**주요어:** CABIN1, T 세포, Calcineurin, NFAT, VIVIT, p38 MAPK

**학번:** 2017-32606